WADC TECHNICAL REPORT 52-243

DAMPING, ELASTICITY, AND FATIGUE PROPERTIES OF TEMPERATURE-RESISTANT MATERIALS

B. J. Lazan
L. J. Demer

Syracuse University

November 1952

Materials Laboratory
Contract No. AF 33(038)-18903
RDO No. 614-16

Wright Air Development Center
Air Research and Development Command
United States Air Force
Wright-Patterson Air Force Base, Ohio

FOREWORD

This report was prepared by Syracuse University under Contract No. AF 33(038)-18903 with Wright Air Development Center, Wright-Patterson Air Force Base, Ohio. The work was initiated under Research and Development Order No. 614-16, "Fatigue Properties of Aircraft Structural Materials," and was administered under the direction of the Materials Laboratory, Directorate of Research, Wright Air Development Center, with W. J. Trapp acting as project engineer.

B. J. Lazan and L. J. Demer, authors, are now Professor of Materials Engineering and Research Associate, respectively, at the University of Minnesota.

ABSTRACT

The damping, elasticity and fatigue properties of several temperature-resistant materials were investigated in rotating cantilever-beam testing equipment. The room and elevated temperature tests were designed to reveal changes in damping energy and dynamic modulus of elasticity during constant cyclic stress fatigue tests at engineering stress levels. Usual S-N fatigue curves are presented in addition to a series of new diagrams designed to show the effects of both stress magnitude and stress history on the damping and elasticity properties. Two methods for comparing the damping energies of a group of materials are offered and the merits of each discussed. Diagrams are also presented to facilitate comparison of the elasticity properties among materials tested at a given temperature.

PUBLICATION REVIEW

This report has been reviewed and is approved.

FOR THE COMMANDING GENERAL:

M. E. SORTE
Colonel, USAF
Chief, Materials Laboratory
Directorate of Research

TABLE OF CONTENTS

LIST OF TABLES

LIST OF ILLUSTRATIONS

INTRODUCTION

Most of the data which have been reported in the literature on the damping and dynamic modulus of elasticity properties of metallic engineering materials were secured either under conditions of very low constant stress or else under conditions of varying stress magnitude and stress history. To be of greatest usefulness in the development and selection of materials as well as for machine design purposes, the data should be obtained from tests conducted under constant stress conditions at levels of practical engineering importance. Furthermore, the important variable of stress history should be carefully controlled.

The work reported in this paper is part of a long-range test program of the above type dealing with the damping, elasticity and fatigue properties of materials at engineering stress levels. It follows an intensive investigation of the properties of mild steel (1)* and includes tests on a number of temperature-resistant materials carried out both room and elevated temperatures.

Objectives and Engineering Importance

The increasingly rapid pace of development in gas turbines, propulsion engines and other high temperature applications has emphazised the importance of a better understanding of the mechanical properties of temperature-resistant materials. Data on the elevated temperature properties under dynamic forces are particularly inadequate. This fact combined with uncertainty as to what constitutes service, makes design engineering in this field particularly difficult. As a consequence there have been many cases of underdesign with resultant service failure, and no doubt there exist the less spectacular but equally costly errors of overdesign with resultant inefficiency due to failure to utilize fully the properties of materials.

One of the least understood of the dynamic mechanical properties is damping. Not only are there practically no engineering data on the damping properties of temperature-resistant materials at elevated temperatures, but the interpretation of these few data is generally quite difficult. Consequently, the significance of damping and its utilization by the engineer for design and failure analyses purposes is generally ignored.

The dynamic modulus of elasticity and its change under sustained cyclic stress is another property of importance to design engineers. An attempt is made, therefore, to present in this paper not only new data on the damping, elasticity modulus and fatigue properties of materials but also to discuss the interpretation, significance and interrelationships of these data.

---

* The bold face numbers in parentheses refer to the list of references appended to this report, see p. 36

PROCEDURE

The experimental data presented in this paper were procured with newly developed rotating-beam equipment which enables continuous measurement of the damping energy and dynamic modulus of elasticity during the course of a rotating-bending fatigue test. Engineering data on the following three dynamic properties of engineering materials are therefore presented and analyzed:

1. Damping energy as a function of stress magnitude and stress history,
2. Dynamic modulus of elasticity as a function of stress magnitude and stress history, and
3. Rotating-bending fatigue strength.

The general engineering importance of these three dynamic properties has been discussed briefly. However these properties assume special significance, as discussed below, when concerned with temperature-resistant materials used in turbine blades and other heat engine parts.

Damping Energy

The damping properties of a material may be defined in several different ways. In this paper damping is specified in terms of damping energy absorbed by one cubic inch of the metal during one complete cycle of vibration. This energy is represented by the area within the stress-strain hysteresis loop as discussed in previous publications (1,6). The engineering importance of damping energy in general machine design, and consequently in the development, selection and processing of engineering materials, has been discussed (3).

Of the several advantages of high damping energy, probably the most important in turbine and heat engine design is that related to the limitation of stress due to near-resonant vibrations. In modern turbines and other high-speed heat engines, near resonant vibrations are generally rather difficult to avoid. It is commonly believed that the increased and uncontrolled stress resulting from these non resonant vibrations constitute one of the more common causes for service failure (5).

The amplification in stress resulting from near-resonant vibrations is reciprocally dependant on the total effective damping capacity of the entire system partaking in the vibration. This relationship may be expressed as follows:

Alternating stress at resonance
=(alternating stress applied externally) X (K_r/D_o) .....(1)
=(alternating stress applied externally) X A_r .....(2)

where:

D_0 = damping energy absorbed by *system* in units of in-lb per cycle of vibration,

K_r = constant depending on the system, and

A_r = resonance amplification factor, unitless = a direct measure of the increase in stress attributable to the resonant condition of a vibration.

The above discussion is in terms of the behavior of a "system." The damping of a system includes not only (*a*) the *internal* hysteresis damping of the material making up the system, but also (*b*) the *external* damping of joints, air friction, dash pots, and other units attached to increase mechanical damping. The relative importance of *internal* damping as compared with *external* damping depends, of course, on the system. It is generally believed, although there is practically no substantiating data, that in most cases external damping is larger than internal damping. However, there is little doubt that in some systems the source of practically all the damping is internal hysteresis. A testing program now in progress at the University of Minnesota is designed to evaluate the relative importance of the various components making up the total damping in different types of systems. However, this paper is concerned entirely with internal hysteresis damping and excludes consideration of extraneous or external damping. This should not be considered a serious limitation since the study of hysteresis damping constitutes a necessary first step. Furthermore, even in cases where there is considerable extraneous damping, high internal damping is still very helpful in limiting near-resonant vibrations.

Different materials possess widely different damping capacity. In some materials at engineering stress levels, the resonance amplification factor may be as high as 1000; in others, as low as 5. Most practical cases, however, lie in the range from 5 to 100 at stresses near the fatigue limit.

In choosing a material for a part which may receive near-resonance vibration in service, it is usually unjustified to use fatigue strength as the main criterion for judgment; the damping must also be considered. For example, Föppl (7) has stated that "the endurance of (airplane propeller) blades depends far more on damping capacity of the material than its fatigue strength." Similarly, overhead cables and aircraft parts made of a low-strength, high-damping material may outlast others made of a high-strength, low-damping material. This relationship of the fatigue and damping properties to the destructive effect of resonant vibration is further discussed in connection with the experimental data presented later.

Dynamic Modulus of Elasticity:

The dynamic modulus of elasticity is defined (1, 6) as the slope of the secant line between the zero and the maximum stress-strain point in the hysteresis loop present during cyclic stress. Stated differently, it is the ratio of the maximum stress to the maximum strain during the cycle. The general significance of dynamic modulus and reasons for its variation during sustained cyclic stress have been discussed elsewhere (1, 4, 6). In so far as turbine blades and other high-temperature applications are concerned, dynamic modulus is considered primarily because of its direct effect on:

(*a*) the position of the resonant frequency spectrum of a part with respect to its operating speeds and

(*b*) the amplitude of vibration of a part, either near to, or remote from, resonance under a given exciting force.

In connection with the first of these considerations, it is generally desirable to design a part so that the lowest critical frequency of its resonant frequency spectrum is above the operating speed of the machine or its serious harmonics. If this cannot be done, which is usually the case in turbine blades, etc., the part is designed so that the operating speed lies between two of the lower critical speeds of the part. In such cases only transient resonant vibrations during "speed-up" need generally be considered rather than the more destructive steady state resonant vibrations. Needless to say, any change in dynamic modulus of elasticity such as occurs during sustained cyclic stress will shift the resonant frequency spectrum and change the "spread" between the operating frequency and one of the resonances. The resultant near-resonant vibrations that may be so developed during prolonged service may, of course, be quite destructive. The importance of knowing dynamic modulus as a function of not only stress but also stress history is thus apparent.

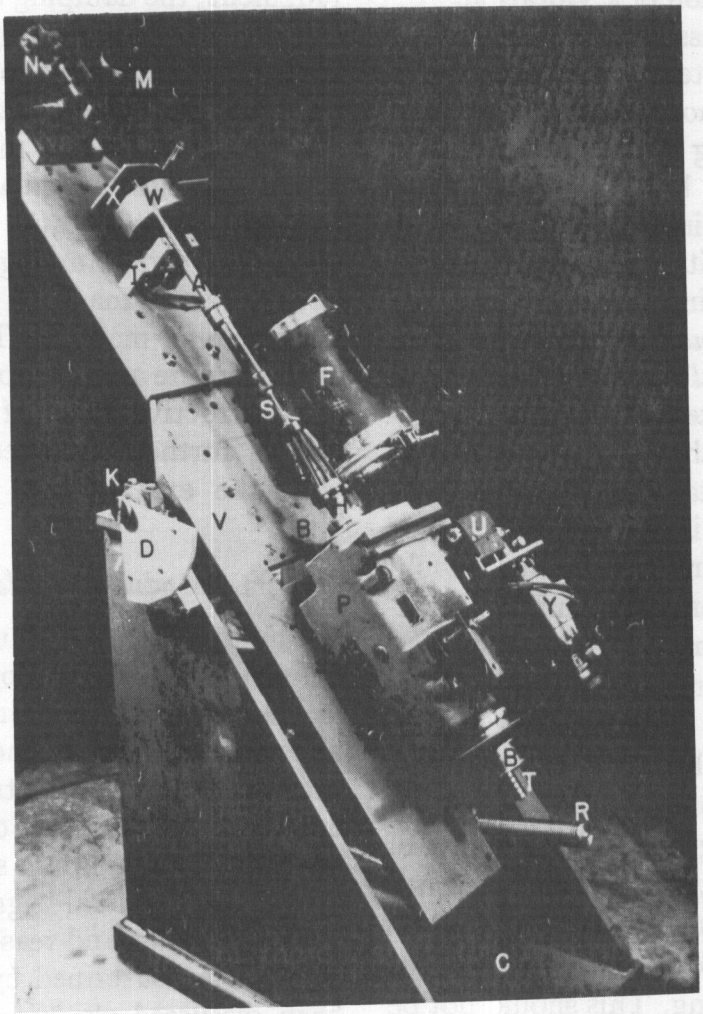

FIG. 1.—Damping, Elasticity and Fatigue Machine for High Temperature Testing.

As in the case of damping, the resonant frequencies for a given design depend not only on the material, but also on the joints and other structural factors. However, as mentioned previously, a knowledge of the behavior of the material is a necessary first step.

Fatigue Strength:

The implications of fatigue stress are relatively well known and need not be reviewed at this time. It should be emphasized, however, that service failure records (5) indicate that fatigue stress in turbine blades constitutes a major cause of breakdown. In this connection, the relationship of magnitude of fatigue stress to the damping properties and proximity to resonance as determined by the dynamic modulus should be reemphasized.

It is thus apparent from the above discussion of damping, dynamic modulus, and fatigue strength that these three properties are not only important individually, but also their interrelationships have considerable engineering significance.

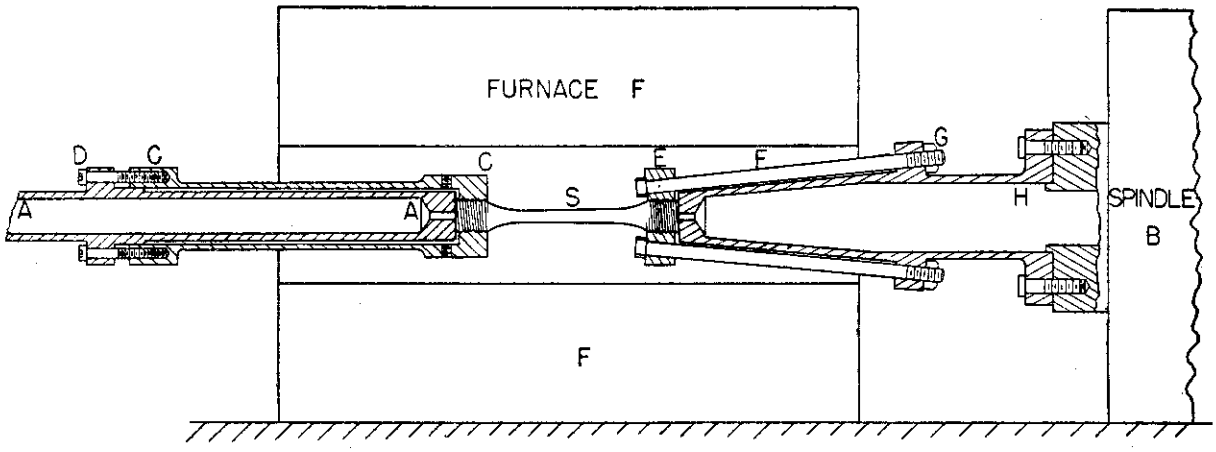

FIG. 2.—Schematic Diagram of Elevated Temperature Gripping System for Rotating-Bending Machine.

TESTING EQUIPMENT, PROCEDURES, AND METHODS OF COMPUTING DATA

Recently developed (1, 4) rotating cantilever-beam equipment was used in this program to procure damping and dynamic modulus data as a function of stress magnitude and stress history. Two of the room temperature models of this machine were converted for elevated temperature testing as shown in Fig. 1. A heavy base *C* with vertical sides *G* supports pillow blocks *K* through which passes a shaft attached to table *V* allowing the table to be tilted about a horizontal axis. The tiltable table supports spindle *B-B* which is mounted in accurate bearings contained in housing *P*. Electric motor *Y* rotates the spindle through a belt drive and also operates a revolution counter *U*. An extension arm-specimen-loading weight assembly *H-S-A-W* is attached to the spindle and rotates with it. During this rotation the horizontal and "vertical" location of a target in the top end of arm *A* may be measured with micrometer slide and microscope assembly *M-N*. A damper disk attached to the upper end of arm *A* through a rounded brass bushing rides on damper plate *X* and eliminates high frequency vibrations of the arm which would make accurate reading of the target position difficult. The damper plate lends no support to the arm and weight assembly. A bracket *I* serves to catch the arm and weight assembly *A-W*, and a microswitch attached to this bracket interrupts the power to the driving motor and furnace when the specimen *S* fractures at the end of a fatigue test. Furnace *F*, when in its proper location, surrounds the specimen and parts of the adjoining extension arms. Thermocouples are attached to the specimen for indication and control purposes. Leads from the thermocouples are directed through the hollow grips and hol-

low spindle B, and by use of slip rings T and a brush assembly (not shown) are connected to a temperature controller. The reversed bending stress to which the test specimen S is subjected is proportional to the sine of the angle between table V and the vertical direction. This angle, indicated on scale D, is steplessly adjustable by means of screw R which is mounted on the base and attached to the lower end of the table.

The method of gripping specimen S within furnace F is shown in Fig. 2. Extension arm H, attached to spindle B, is made hollow so as to minimize heat transfer from the furnace to the spindle bearings. The bottom end of the specimen is held rigidly against arm H by nut E and studs F, the pre-load in the assembly being large so as to avoid relative motion within the grip with consequential fretting and energy loss. The threaded left end of the specimen is similarly held against loading arm A by sleeve-nut combination C, preloaded by means of screws D. The arm-specimen assembly S-A is carefully lined up on dead centers by preferentially tightening the various holding and adjusting screws prior to attachment to the spindle. The assembly is then attached to the spindle extension arm H at room temperature and adjusted to run true by means of preferentially tightening nuts G on studs F. The furnace is then placed in position down over the loading arm and the weight W is mounted on the arm.

Even though the specimen-arm assembly is adjusted to run true on the spindle at room temperature, it is frequently found that the run-out of arm A and its measuring target may become significant after the assembly reaches the testing temperature. In such cases, nuts G are again preferentially tightened after the temperature has stabilized to make the measuring target again run true.

The gripping method employed permits use of relatively simple threaded specimens. Considerable leeway in accuracy is allowed in the threaded ends since the alignment adjusting system described above compensates for thread errors. Furthermore, preloading the threaded connections eliminates backlash and the accompanying fretting corrosion. Consequently, the "frozen" joint condition, which frequently occurs in fatigue testing at elevated temperatures, is practically eliminated.

For the measurement and control of specimen temperature, leads from three thermocouples spaced at the top, middle, and bottom of the specimen test length were carried through chromel and alumel slip rings and brushes to the temperature controller and indicating potentiometer. The maximum variation in temperature between the bottom and top of a specimen and the variation in temperature at a station during a complete test were in most cases about $\pm$ 10 F.

All tests were conducted at about 20 rpm for the first 500 cycles of stress. As a rule, the speed was then changed to 50 rpm until several thousand cycles were reached after which the highest speed between readings was about 150 rpm for the elevated temperature tests and various speeds up to 1000 rpm for the room temperature tests. In all cases the speed of reading was the same—20 rpm. Previous investigations (1, 6) have shown that damping and dynamic modulus of elasticity are frequency sensitive at room temperature. This is also true at elevated temperatures. However, at least at room temperature, the frequency of stress history does not affect the actual damping or modulus values that will be obtained after a given number of stress cycles.

Other details on testing equipment and procedures are described in previous publications (1, 4).

As indicated in the publications just referred to, the damping energy and dynamic modulus may be determined from the following relationships:

$$D = K\,(SH) \quad \ldots\ldots\ldots\ldots\ldots\ldots (3)$$

$$\text{and } E_d = C\,(S/V) \quad \ldots\ldots\ldots\ldots\ldots\ldots (4)$$

where:

D = damping energy absorbed by the specimen, in-lb per cu in. per cycle of stress,

E_d = dynamic modulus of elasticity (secant value) during reversed-bending stress, psi,

S = amplitude of reversed stress in specimen, psi,

V = "vertical" (gravitational) deflection of the target T (toward table V in Fig. 1) due to bending stress in the specimen, in.,

H = horizontal traversal of the target T or its total lateral displacement (perpendicular to the direction of its gravitational deflection) caused by reversing the direction of rotation of the spindle, in., and

K and C = constants dependent only on specimen shape, weight, and center of gravity of the loading arm assembly, and the location of the target along the axis of the loading arm.

The method for evaluating the K constant in Eq 3 was the same as that discussed previously (1). For the tests reported in this paper, the initial room temperature static modulus of elasticity was determined for a given material by comparing the low stress deflection of the target under very slow rotation (less than 20 rpm) for specimens of that material with the corresponding deflections obtained with specimens of type 403 stainless steel having the same dimensions. The static modulus of elasticity value for type 403 was obtained from the results of a standard axial static tension test. The elevated temperature static modulus for a given material was determined by comparing the low stress deflections of the target under very slow rotation at test temperature with corresponding deflections measured at room temperature for the same specimen. Since for some of the powder metals studied in this program variations of about 5 per cent were observed in the static moduli of elasticity due to inhomogeneity of the material, the C constants in Eq 4 were determined as follows in order to unify the data and more readily reveal trends. Using Eq 6

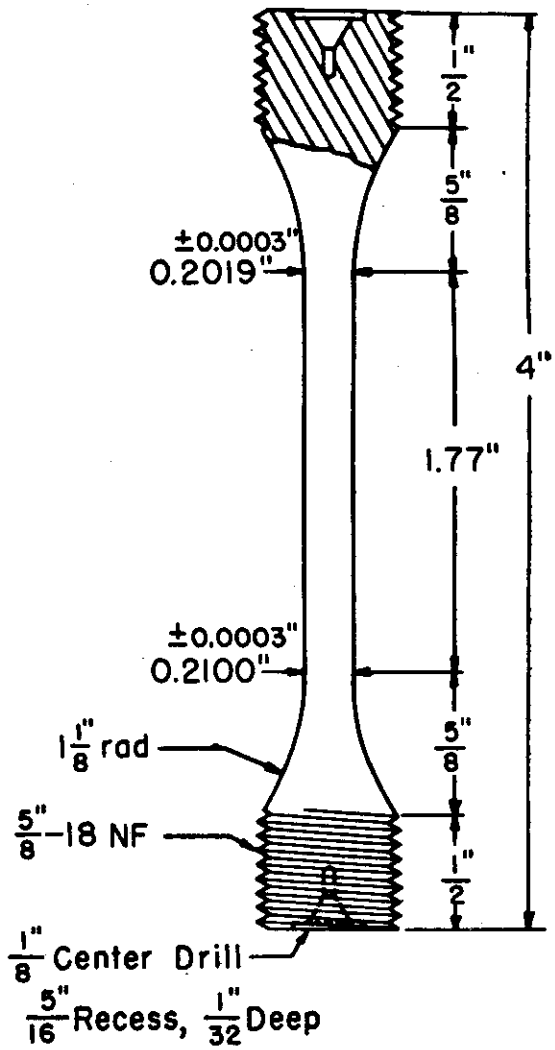

FIG. 3.—Type E Specimen for Damping, Elasticity, and Fatigue Testing.

in Reference (1), the dynamic modulus, E_d was calculated at a given stress history from the known values of E_s, D, and S. The corresponding vertical deflection, V, at this stress history was used in Eq 4 to determine C. This value of C was used thereafter at all stress histories to calculate the dynamic modulus from the vertical deflection values.

TABLE I.—CHEMICAL COMPOSITION, PRODUCTION, AND TREATMENT.

Alloy	Chemical Composition, per cent																Production and Heat Treatment
	Carbon	Manganese	Phosphorus	Sulfur	Silicon	Nickel	Chromium	Molybdenum	Tungsten	Cobalt	Columbium	Iron	Aluminum	Titanium	Copper	Nitrogen	
S-816 (Material D)	0.40	0.70	0.014	0.016	0.51	20.68	19.79	3.46	4.46	43.40	3.80	2.50	...	...	...	...	Wrought bar stock 1⅝ in. diameter. Solution treatment—2150 F for 1 hr—water quenched. Aging treatment—1400 F for 16 hr—still air cooled.
Inconel X (Material E)	0.40	0.51	...	0.007	0.39	73.16	14.61	...	...	...	1.04	6.87	0.88	2.44	0.03	...	Wrought bar stock 1¾ in. diameter. Solution treatment—2000 F for 2 hr—fan air cooled. First aging—1550 F for 24 hr—still air cooled. Second aging—1300 F for 20 hr—still air cooled.
Type 403 (Material F)	0.12	0.37	0.016	0.022	0.26	0.44	12.67	...	...	...	...	86.1 (bal)	...	...	...	...	Wrought bar stock 1¾ in. diameter. Hardening treatment—1700 F for 15 min—fan air cooled. Tempering treatment—970 to 1020 F for 2 hr—air cooled. (Drawn to 30 to 36 Rockwell C)
Low Carbon N-155 (Material NA)	0.15	1.74	...	...	0.37	19.4	21.7	2.76	1.90	19.0	0.76	32.1 (bal)	...	...	...	0.14	15.5 in. ingot hammer cogged to 2-in. squares. Rolled to 1-in. rounds at 2050 to 1830 F. Water quenched from 2200 F. Aging treatment—1400 F for 16 hr—air cooled.
TP-2-R (Material G)	...	...	...	...	...	...	...	100	...	...	...	...	...	...	...	...	Pure molybdenum powder containing microscopic traces of impurities, cold pressed and sintered in hydrogen bell, swaged to bar stock ⅞-in. diameter, forged to ⅝ in. flat between parallel dies. Annealing treatment—1750 F for 4 hr—hydrogen atmosphere.
TP-2-B (Material G_a)	...	...	...	...	...	...	...	98	2	...	...	...	...	...	...	...	Molybdenum with 2 per cent tungsten arc-cast (6-in. diameter). Hammered to 2⅝-in. diameter billets, rolled to ⅞-in. diameter, forged to ⅝-in. flat between parallel dies. Annealing treatment—1750 F for 4 hr—hydrogen atmosphere.
TP-1-2 (Material H)	...	...	...	...	...	...	...	...	...	...	...	85[a]	...	...	15[a]	...	High purity iron powder (approximately 98.5 per cent pure) cold pressed, sintered, coined, and "infiltrated" with a molten copper alloy to obtain 100 per cent density. Iron contained following approximate impurities before sintering: C..... 0.03 per cent; P..... 0.006 per cent; Mn..... 0.4 per cent; Oxides..... 1.0 per cent; Si..... 0.1 per cent. TP-1 material given standard solutions and aging treatment to obtain maximum tensile strength.
TP-1-3 (Material HA)	...	...	...	...	...	...	...	...	...	...	...	85[a]	...	...	15[a]	...	Same as TP-1-2 material but giving modified solution and aging treatment to obtain high ductility.

[a] Approximate.

Design and Preparation of Test Specimen

The test specimen utilized in this work is shown in Fig. 3. The tapered test section is so designed as to produce equal maximum bending stress along the length of the test section under the cantilever loading. In the interest of uniformity of stress, it is also desirable to use hollow, thin-walled specimens (1). However, specimen preparation difficulties for several of temperature-resistant materials necessitate use of the small, solid specimens shown. Since in these solid specimens all stresses from zero to maximum are always present, the damping energy determined is an average value for stresses between zero and maximum.

Final polishing of the specimens was done in a special abrasive belt machine (8).

Test Materials and Program

The test materials used in this program and the testing temperatures for each are given below:

S-816	Room temperature, 900 F and 1600 F
TP-2-R	Room temperature and 900 F
TP-2-B	Room temperature and 900 F
Type 403	Room temperature and 500 F
TP-1-2	Room temperature and 500 F
Inconel X	Room temperature
Low carbon N-155	1500 F

The above elevated temperatures were selected for the tests because 500 F is close to the average temperature of the blades in the compressor section of a jet engine, 900 F is about the highest temperature that can be used with the TP-2 materials without using a protective atmosphere, and 1600 F is the approximate operating temperature of the blades in the turbine section of a jet engine. There is considerable creep data available for N-155 at 1500 F; hence, the selection of that test temperature.

Chemical compositions, heat treatment data, and static physical properties are given in Tables I and II.

The aims of this investigation were to secure data of engineering value on the dynamic properties of damping, elasticity, and fatigue; to present them in a clear fashion showing the dependence of these properties on certain other variables; and lastly to present methods for the comparison and evaluation of these dynamic properties of materials. An attempt to explain the reasons for the different behaviors obtained and a metallurgical investigation of the types of fracture encountered or the changes taking place in the structure of the materials during the course of the tests are extremely important phases of the entire study that are unfortunately beyond the scope of this present paper.

TABLE II.—STATIC PHYSICAL PROPERTIES.

Material	Temperature, deg Fahr	Yield Strength, 0.2, per cent offset, psi	Tensile Strength, psi	Elongation, per cent	Reduction in Area, per cent	Modulus of Elasticity, psi
S-816	RT	67 000	140 000	35	29	34.0×10^6
	900	55 000	125 000	20	10	29.4
	1600	39 600	59 000	25	30.2	24.0
TP-2-R	RT		75 500	0	0	45
	900	64 500	66 200	12	48	42.7
TP-2-B	RT	104 500	120 000	4.5	4.8	48
	900	67 000	71 000	19	74.5	44.4
Type 403	RT	138 000	152 000	17.5	64	29.0
	500	122 000	139 000	15	60	26.5
TP-1-2	RT	107 000	121 000	2.0	3.0	24.5
	500	89 000	99 500	2.0	4.3	23.0
TP-1-3	RT	65 000	77 000	9.7		24.5
	500		67 500	12.5		23.0
Inconel X	RT	92 000	162 000	24	30	31
Low carbon N-155	1500	35 800	44 600	23	27	

Test Data

Records of the damping and elasticity data kept during the course of constant stress rotating-bending fatigue tests of a given material afford information from which basic diagrams of the type shown in Figs. 4 and 7 are constructed. Figure 4

is a plot of the original data of damping energy *versus* the number of reversed stress cycles for the tests on S-816 alloy. Each curve represents the data from a single fatigue test of a given virgin specimen (one not previously subjected to stress) brought either to failure in above fatigue strength tests or to several million cycles in below fatigue strength tests.

temperature. By carrying out such a program at different temperature levels, the effect of temperature is determined.

In a manner similar to the above, Fig. 7 presents the dynamic modulus of elasticity data for S-816, showing by means of an E_d-N-S diagram, the effect of stress history and stress magnitude on the dynamic modulus.

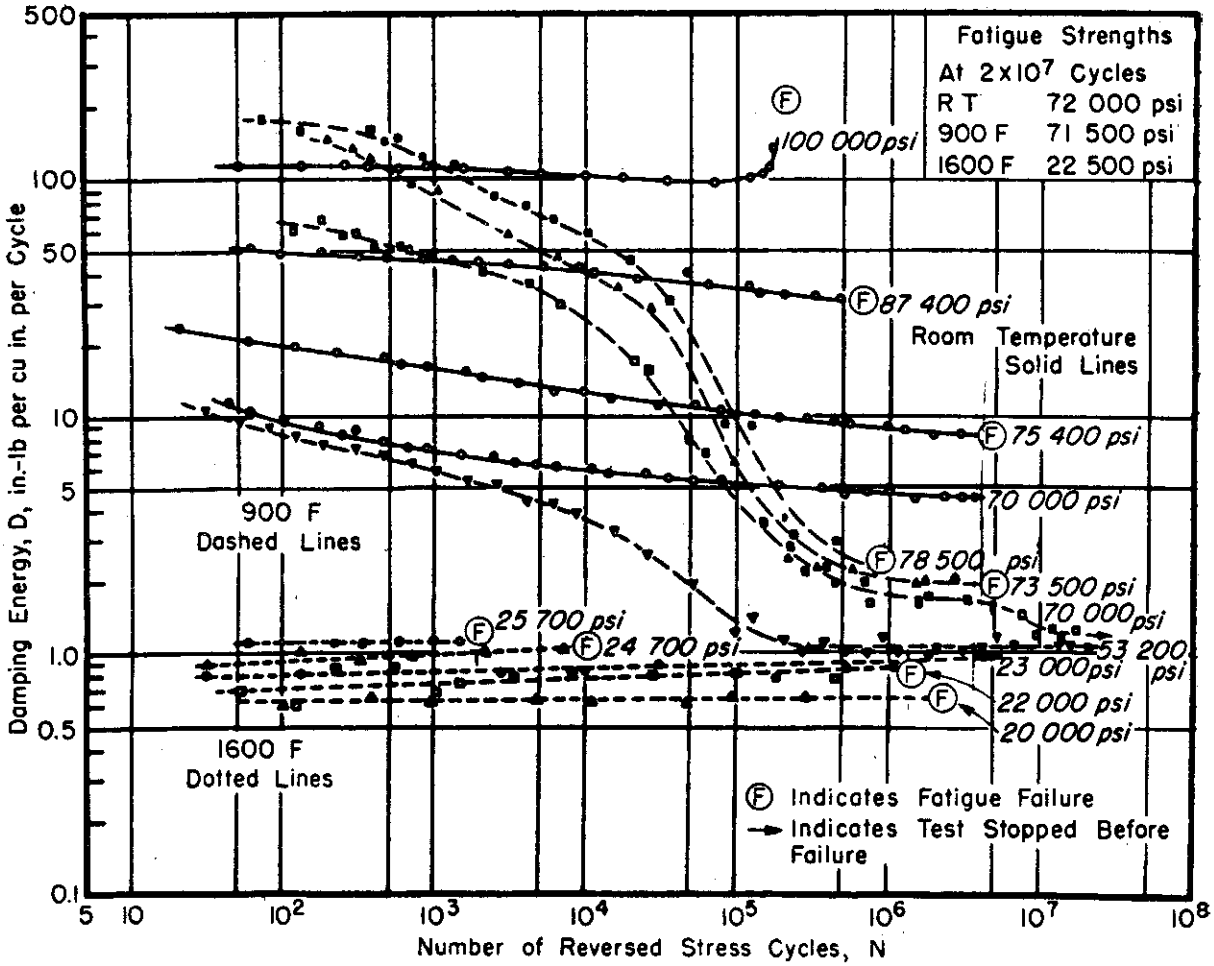

FIG. 4.—*D-N-S* Diagram Showing the Effects of Several Magnitudes of Sustained Reversed Stress on the Relationship Between Damping Energy and Number of Cycles for S-816 Alloy (Material D) at Room Temperature, 900 F, and 1600 F.

Thus, each curve shows the effect of number of cycles, N, in the stress history on the damping energy, D, during a test at constant reversed bending stress, S. By testing other specimens, each at a different stress, the dependence of damping on stress magnitude is obtained. The series of curves represents a so-called *D-N-S* diagram for the material at that

Figure 22 presents usual *S-N* fatigue curves for the results of room temperature and elevated temperature tests of all materials.

The other diagrams presented in this paper were prepared by replotting and combining in different ways the original damping, elasticity, and fatigue data secured at the various temperatures. These

new diagrams are intended to increase understandability and usability in design and in material comparison studies.

It should be emphasized at this point that the entire testing program was designed to be exploratory in nature. Only a few specimens of each material were presented involve, in some cases, extrapolating and smoothing out of the original data obtained. Therefore, the values and patterns indicated should, in some cases, be considered qualitative and comparative studies rather than precise quantitative data.

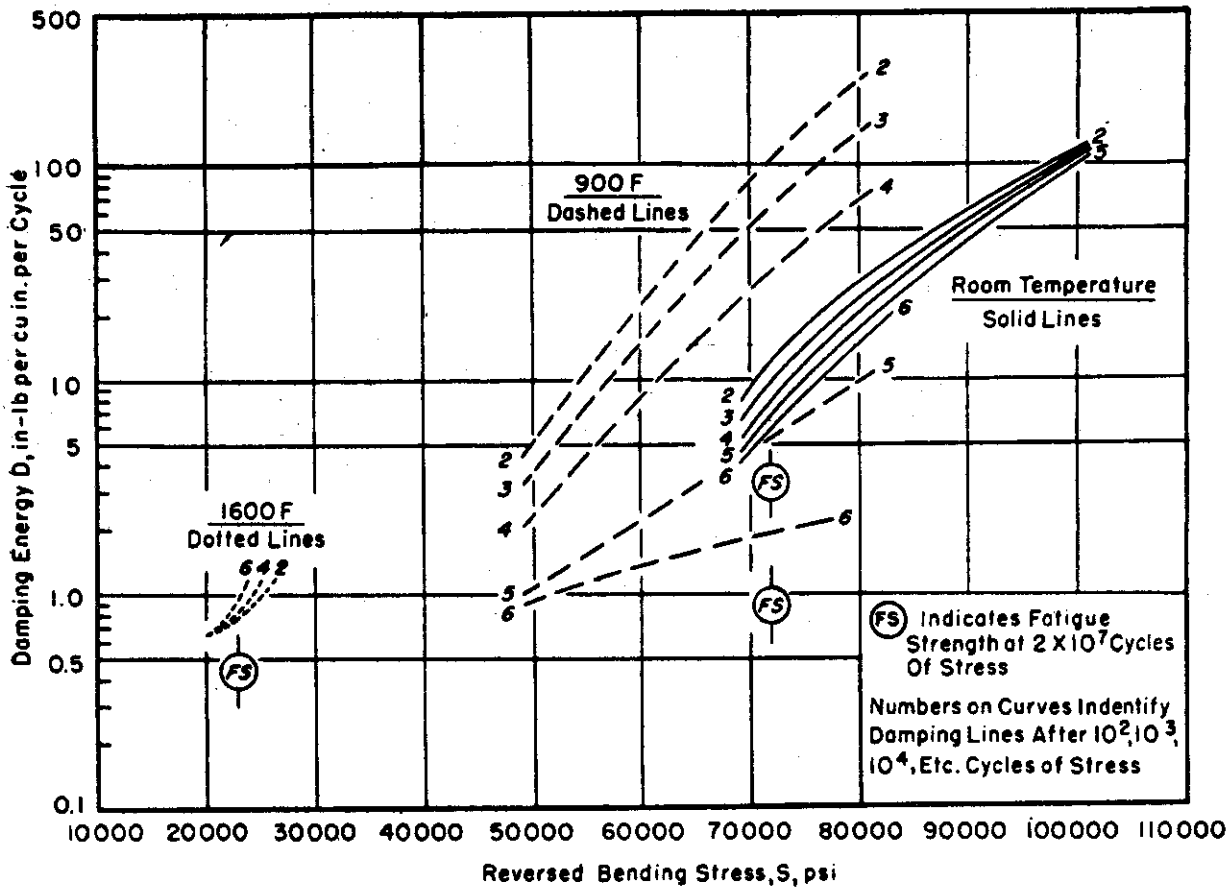

FIG. 5.—*D-S-N* Diagram Showing the Effects of Several Numbers of Sustained Reversed Stress Cycles on the Relationship Between Damping Energy and Stress Magnitude for S-816 Alloy (Material D) at Room Temperature, 900 F, and 1600 F.

tested at a given temperature to obtain the damping, elasticity, and fatigue data. It is felt that since so little is known regarding damping and related dynamic properties, exploratory tests on several materials are more revealing than an equal effort spent on an intensive study of one of these materials. That this extensive rather than intensive approach was desirable is indicated by the wide variety of behavior patterns displayed by the various materials.

It should be pointed out also that the fatigue, damping, and elasticity diagrams

DISCUSSION OF DATA

Damping, Elasticity, and Fatigue Properties:

Figure 4 is presented as a typical *D-N-S* diagram in order to show a complete set of original damping data. The plot is of particular interest because this material, S-816, was tested at three different temperatures and also because the curves (at 900 F) display greater changes in damping energy with stress history than do those for any of the other materials tested. The room temperature data

shown in solid lines indicate a definite decrease in damping with increasing number of cycles until fracture occurred for all specimens except the one tested at 100,000 psi. This curve displays a sharp upward trend near the end which may be significant since it occurred during a period representing more than half of the which is about 10 per cent above the fatigue strength, the damping decreased from a value of 200 in-lb per cu in. per cycle at 50 cycles to about 2 in-lb per cu in. per cycle at 10^6 cycles of stress, representing a decrease to 1 per cent of its 50 cycle value. At the lower stresses the change is somewhat smaller than this. So

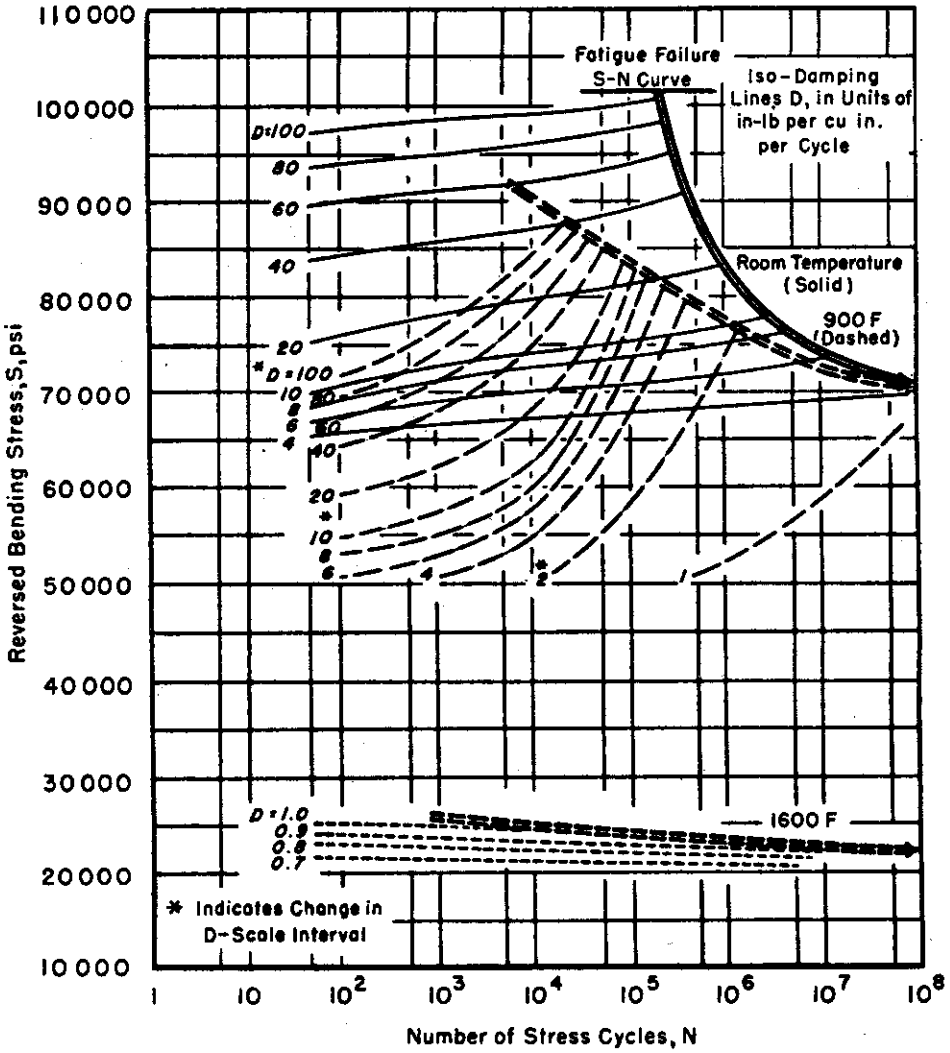

FIG. 6.—*S-N-D* Diagram Relating Stress, Number of Cycles, and Iso-Damping Contour Lines for S-816 Alloy (Material D) at Room Temperature, 900 F, and 1600 F.

life of the specimen (cycles, *N*, plotted logarithmically).

For the tests at 900 F, curves shown as dashed lines, there is an even more pronounced decrease in damping with stress history than at room temperature. The decrease is particularly rapid in the region of 10^4 to 10^6 cycles of stress. For the specimen tested at a stress of 78,500 psi, that time at temperature (900 F) is not thought to be the sole cause of this decrease, it should be noted that the aging treatment for this material consisted of 16 hr at 1400 F followed by still air cooling. Furthermore, when the specimen tested at 53,200 psi at 900 F (which did not break in more than 10 million cycles) was retested at a higher stress, a curve

similar in shape to those for the virgin specimen was obtained. The rapid decrease in damping again occurred at about the same number of cycles.

The damping data for 1600 F shown as dotted lines in Fig. 4 display little change with stress history exhibiting only a slight *increase* as the number of cycles becomes larger. The specimen at 20,000 psi which is below the reported fatigue strength at 1600 F was overheated before testing and it is thought that this adversely affected its life.

It should be pointed out that the damping values do not always decrease with an increase in number of cycles at room temperature. Many different patterns of behavior have been observed; for example, the damping for TP-2-B increases continuously with an increase in the number of cycles; type 403 displays an initial decrease followed by an increase to a peak after which the values decrease if the specimen does not previously fracture. The data for TP-1-2 show damping values decreasing to a minimum followed by a steady increase to fracture; material TP-1–3 displays practically no change in damping with number of cycles; and Inconel X has very high initial damping followed by a period of practically no change after which the damping increases sharply till failure. The general trends for a given material may be the same at elevated temperature as at room temperature, as in the case of TP-2-B for room temperature and 500 F, or they may be reversed as in the case of S-816 at room temperature and 1600 F. Qualitative indications of these trends are discussed later in connection with the *S-N-D* diagrams presented.

The data for S-816 diagrammed in Fig. 4 are replotted in Fig. 5. This diagram shows damping, D, at three temperatures as a function of the magnitude of reversed bending stress, S, with lines marked 2, 3, 4, 5, and 6 connecting the damping values after 10^2, 10^3, 10^4, 10^5, and 10^6 cycles, N, of stress. This *D-S-N* diagram affords a convenient method for comparing the damping behavior of S-816 at the three temperatures. The flags enclosing the letters F.S. indicate the fatigue strengths of the material. It is interesting to compare the damping values at different temperatures for stresses corresponding to the fatigue strengths. The room temperature damping after 100 cycles at a stress equal to the fatigue strength is about one-fifth that of the damping at 900 F at a stress equal to the 900 F fatigue strength and about twenty times the corresponding value for 1600 F. After 10^6 cycles of stress, the room temperature value is about three times the corresponding 900 F value and about six times that at 1600 F.

A method of showing the fatigue properties along with the damping properties for a given material in one diagram is shown in Fig. 6. This presents an *S-N-D* diagram for S-816 alloy showing the data for the three test temperatures. The plot is easily made from the *D-S-N* diagram of Fig. 5. It shows the relationships between the three variables by the use of iso-damping contour lines D on a plot of stress magnitude, S, *versus* the number of stress cycles, N. In Fig. 6 the data for room temperature are shown in solid lines, those for 900 F in dashed lines, and those for 1600 F in dotted lines. The double curve in each case represents the fatigue failure *S-N* curve.

In interpreting an *S-N-D* diagram, the rules relating to contour lines of elevation on a topographic map are useful. For example, in proceeding toward the right in Fig. 6 along a constant stress line, the crossing of iso-damping lines of successively lower values for both room temperature and 900 F data indicates a downhill trend in damping energy. Conversely, with the data for 1600 F, an uphill trend is seen in damping energy at

constant stress as the number of stress cycles is increased. These behaviors are, of course, merely another method for showing the trends indicated in the plot of Fig. 4.

Of additional interest in Fig. 6 is the observation that the fatigue strength for 20 million cycles at 900 F is practically the same as the room temperature value, but the 1600 F fatigue strength is only about one-third of the room temperature value.

As pointed out in a previous paper (1), the variation of dynamic modulus of elasticity with number of cycles of stress is, in general, reciprocal to the change in damping capacity. Figure 7 is an E_d-S-N diagram for S-816 alloy at the three testing temperatures. Comparing this plot with the corresponding D-N-S diagram of Fig. 4, the general reciprocal relationship mentioned above is apparent. For the specimens tested at room temperature, an increase in dynamic modulus is observed at all stresses except the highest —100,000 psi. This curve shows a decreasing trend to fracture where the value recorded is approximately 80 per cent of the initial modulus value. The data for all of the specimens at 900 F show increasing values of E_d with an increase in number of cycles. The values for a small number of cycles are approximately 70 per cent of the initial static modulus value at 900 F, while the highest indicated are some 3 per cent above this figure. Changes in the static modulus of elasticity after exposure to reversed stress at elevated temperature for a large number of cycles have been determined for S-816. For one specimen at 1600 F, a stress history of one million cycles at 1600 F at a stress slightly below the fatigue strength resulted in an increase of

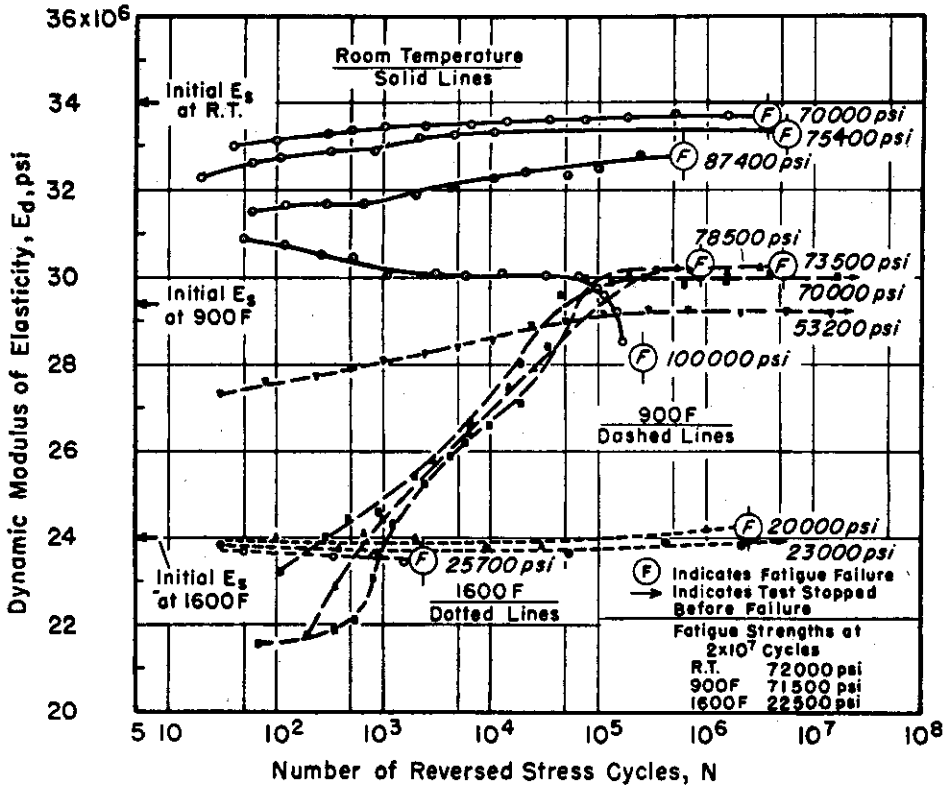

FIG. 7.—E_d-N-S Diagram Showing the Effects of Several Magnitudes of Sustained Reversed Stress on the Relationship Between Dynamic Modulus of Elasticity and Number of Cycles for S-816 Alloy (Material D) at Room Temperature, 900 F, and 1600 F.

slightly more than 1 per cent over the value for the virgin specimen. (For one specimen of N-155 tested at 1500 F at a stress slightly above the fatigue strength, an increase of about 3 per cent in the static modulus was measured after 100,000 cycles of stress.) The fatigue strengths of S-816 at the three temperatures are indicated in the corner of Fig. 7 to provide a measure of the proximity of the test stress to the fatigue strength in each case. The static moduli for the virgin specimens at each temperature are indicated on the left side so that comparisons with the values for dynamic modulus may be made.

The data for the dynamic modulus of S-816 in Fig. 7 are replotted in Fig. 8 as an E_d-S-N diagram to facilitate explanation. The diagram shows dynamic modulus E_d for the three temperatures as a function of reversed bending stress, S, with lines marked 2, 3, 4, 5, and 6 connecting the dynamic modulus values after 10^2, 10^3, 10^4, 10^5, and 10^6 cycles of stress. It shows clearly the large changes in elasticity at 900 F with both stress magnitude and stress history when compared with the smaller changes at the other two temperatures. The F.S. flags are again used to indicate the fatigue strengths at the different temperatures.

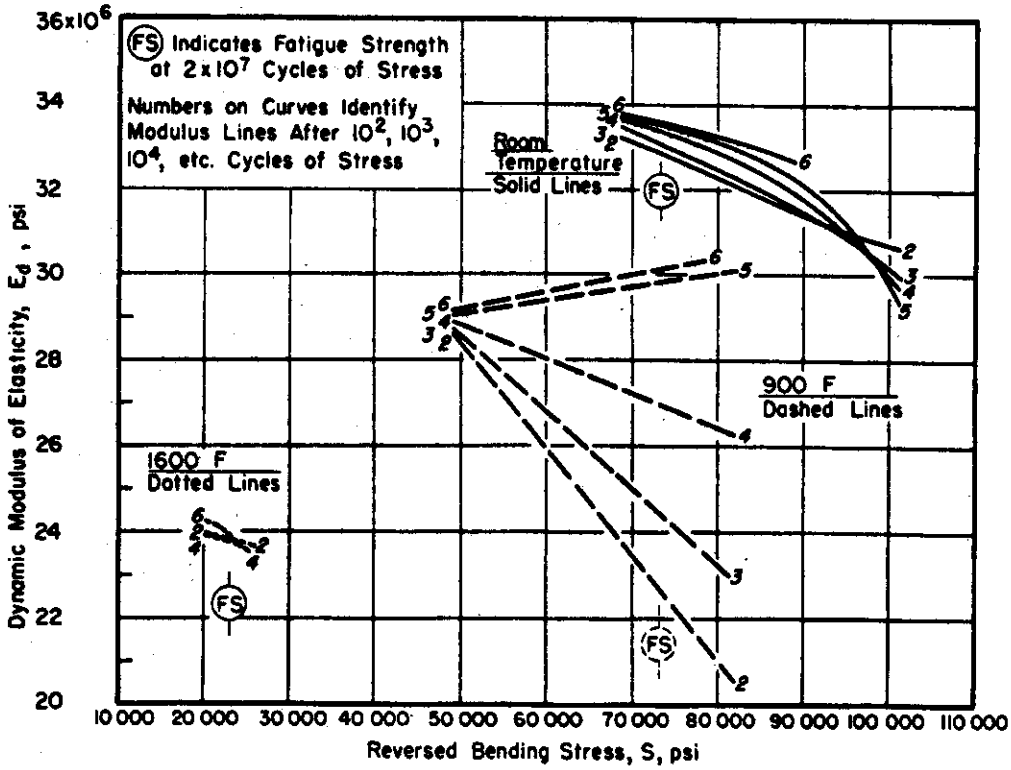

FIG. 8.—E_d-S-N Diagram Showing the Effect of Several Numbers of Sustained Reversed Stress Cycles on the Relationship Between Dynamic Modulus of Elasticity and Stress Magnitude for S-816 Alloy (Material D) at Room Temperature, 900 F, and 1600 F.

The dynamic modulus does not for all materials increase with an increase in the number of stress cycles. There are just as many different trends and patterns in the behavior of this property as in the case of damping energy. However, the reciprocal relationship to the damping values does generally exist.

The summary diagram for the elasticity and fatigue properties for S-816 alloy at the three test temperatures (corresponding to Fig. 6 for the damping and fatigue properties) is the S-N-E_d diagram shown in Fig. 9. This plot shows the relationships between three variables by showing iso-modulus of elasticity contour

lines E_d on a plot of stress magnitude S *versus* the number of stress cycles N. Again solid, dashed, and dotted lines indicate the data for room temperature, 900 F, and 1600 F. The static moduli of elasticity for the virgin specimens at each temperature are presented in the corner of the diagram for comparison purposes. Such diagrams are shown in Figs. 10 and 11 for TP-2-R (pure molybdenum), in Figs. 12 and 13 for TP-2-B (molybdenum plus 2 per cent tungsten), in Figs. 14 and 15 for type 403, and in Figs. 16 through 19 for the TP-1 (copper infiltrated sintered iron powder). Data are presented for each of these materials in-

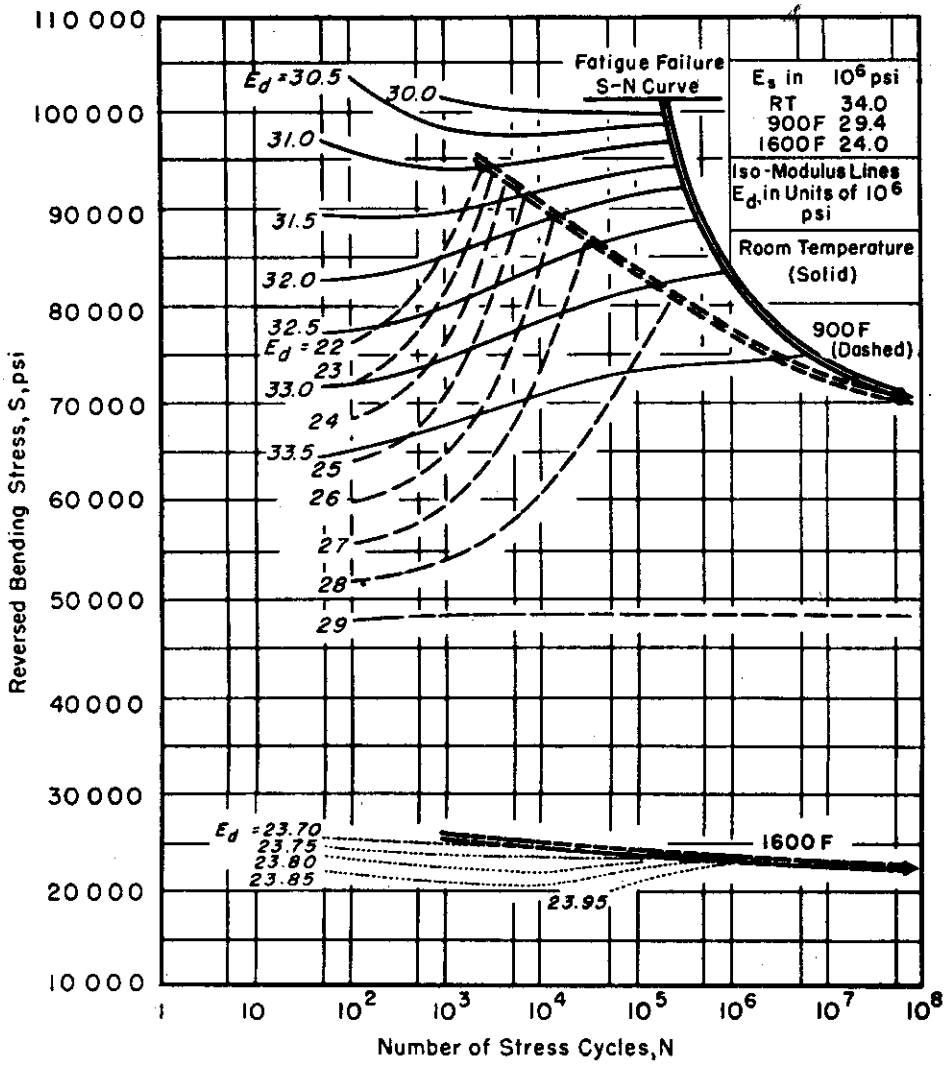

FIG. 9.—S-N-E_d Diagram Relating Stress, Number of Cycles, and Iso-Modulus of Elasticity Contour Lines for S-816 Alloy (Material D) at Room Temperature, 900 F, and 1600 F.

The general trends of the iso-modulus lines are seen to be similar to those of the iso-damping lines in Fig. 6, although the change in elasticity is reciprocal to the change in damping.

Companion S-N-D and S-N-E_d diagrams present the damping, elasticity, and fatigue data for a given material. vestigated at two temperature levels, room temperature and 900 F for three of the materials, and room temperature and 500 F for three others.

The two TP-2 materials display generally similar trends for the iso-damping and iso-modulus lines. Sloping downward to the right, the iso-damping lines indi-

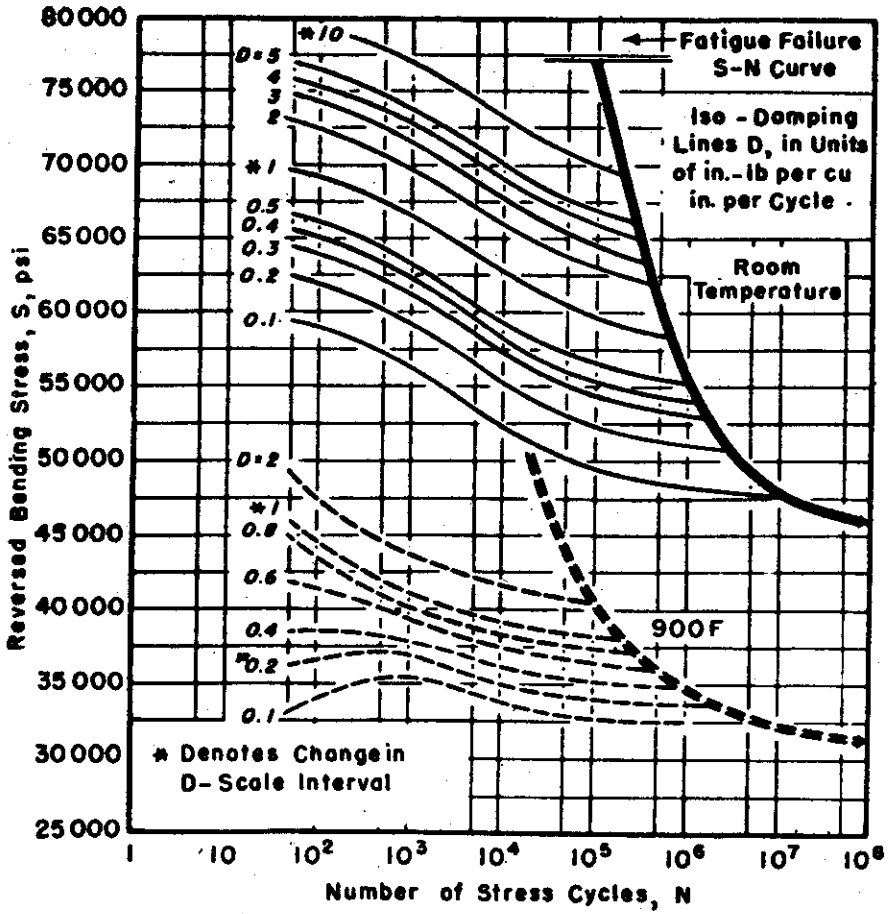

FIG. 10.—*S-N-D* Diagram Relating Stress, Number of Cycles, and Iso-Damping Contour Lines for TP-2-R (Material G) at Room Temperature and 900 F.

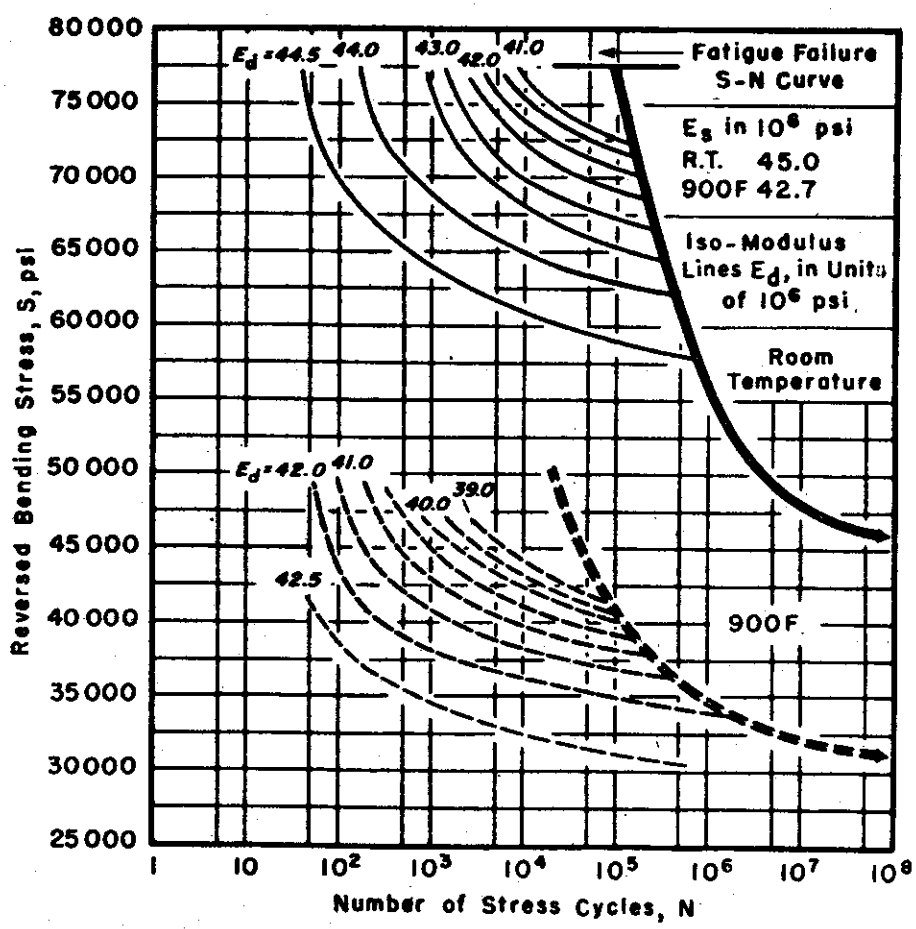

FIG. 11.—*S-N-E*$_d$ Diagram Relating Stress, Number of Cycles, and Iso-Modulus of Elasticity Contour Lines for TP-2-R (Material G) at Room Temperature and 900 F.

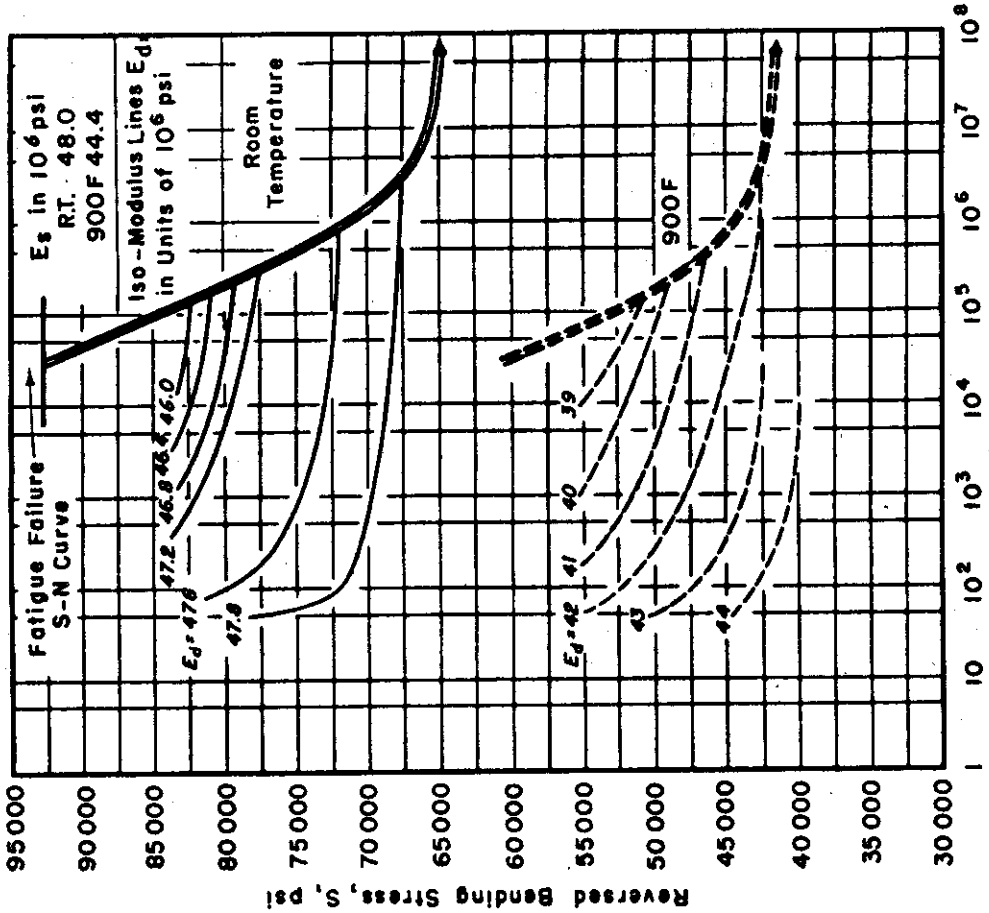

FIG. 13.—*S-N-E*$_d$ Diagram Relating Stress, Number of Cycles, and Iso-Modulus of Elasticity Contour Lines for TP-2-B (Material G_A) at Room Temperature and 900 F.

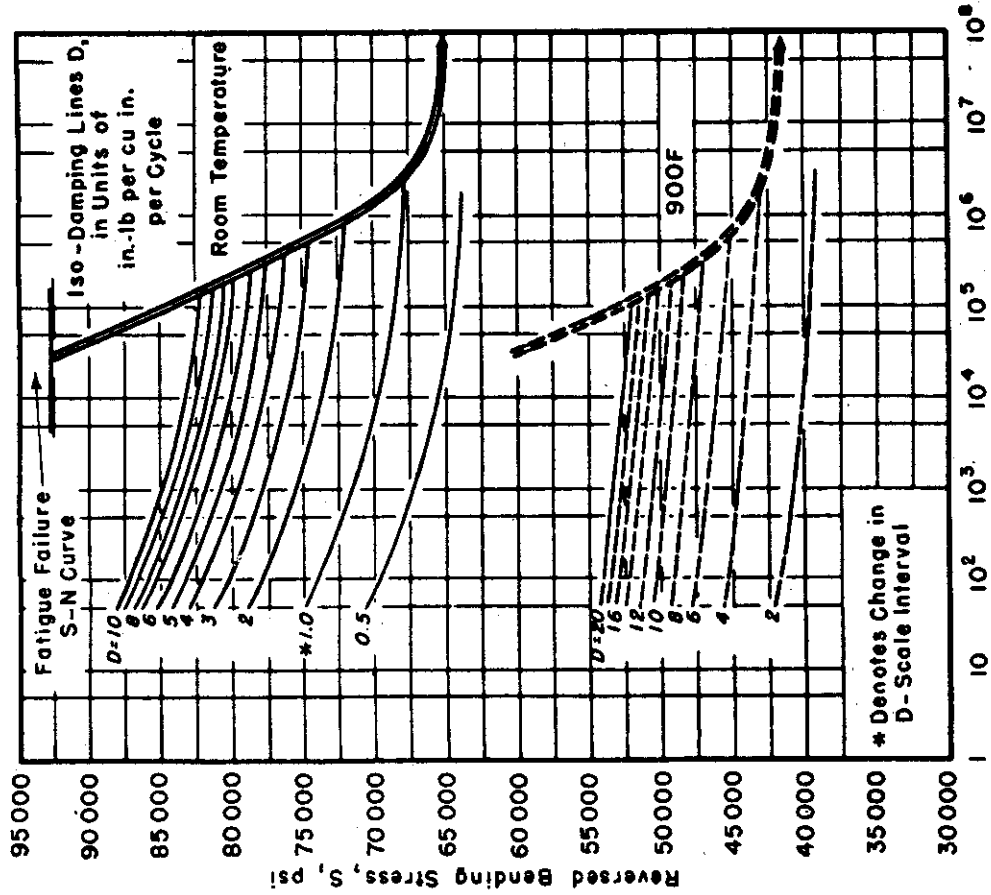

FIG. 12.—*S-N-D* Diagram Relating Stress, Number of Cycles, and Iso-Damping Contour Lines for TP-2B (Material G_A) at Room Temperature and 900 F.

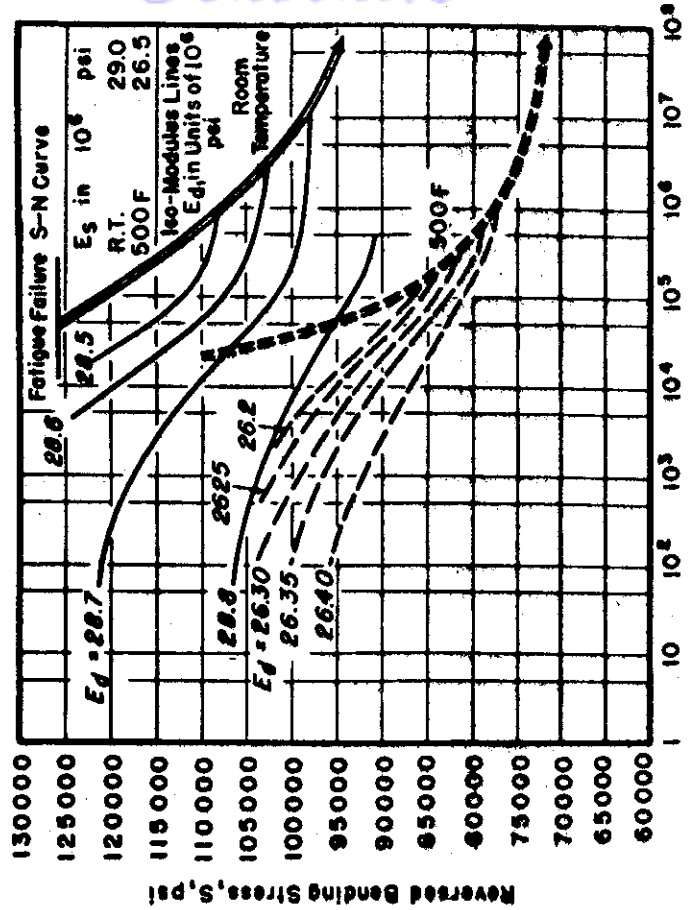

FIG. 14.—*S-N-D* Diagram Relating Stress, Number of Cycles, and Iso-Damping Contour Lines for Type 403 Alloy (Material F) at Room Temperature and 500 F.

FIG. 15.—*S-N-E* Diagram Relating Stress, Number of Cycles, and Iso-Modulus of Elasticity Contour Lines for Type 403 Alloy (Material F) at Room Temperature and 500 F.

cate an uphill trend in damping values during a constant stress test since a constant stress line intersects lines of increasing D values as the number of cycles N increases. The E_d lines also sloping downward to the right indicate a downhill trend in modulus values since a similar stress line intersects iso-modulus lines of lower values with increasing number of stress cycles N. The patterns displayed by type 403 and TP-1-2 are generally similar at both room temperature and 500 F, although the stress levels for corresponding damping values at a given number of cycles are much higher for type 403. The data for TP-1-3 display the least change in damping and elasticity values with number of cycles of any of the materials tested (Figs. 18 and 19). A noteworthy point in connection with the data for the TP-1 materials is that in both cases the fatigue failure curves at 500 F cross over the room temperature curves after about one million

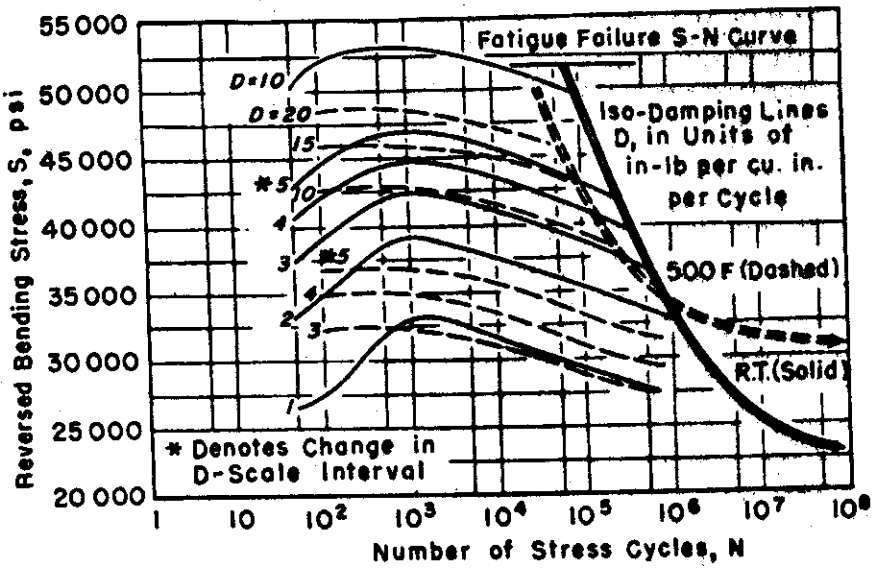

FIG. 16.—*S-N-D* Diagram Relating Stress, Number of Cycles, and Iso-Damping Contour Lines for TP-1-2 (Material H) at Room Temperature and 500 F.

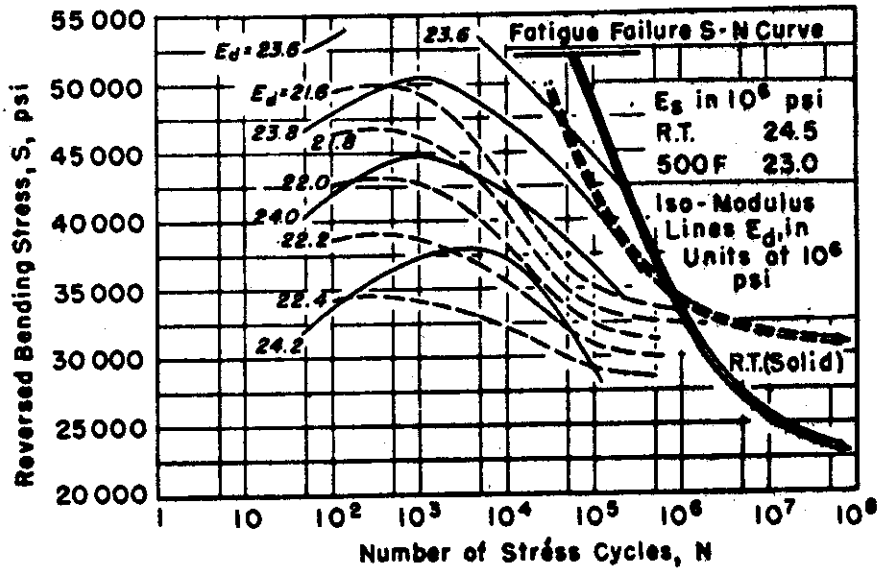

FIG. 17.—*S-N-E*$_d$ Diagram Relating Stress, Number of Cycles, and Iso-Modulus of Elasticity Contour Lines for TP-1-2 (Material H) at Room Temperature and 500 F.

cycles so that the fatigue strengths at 20 million cycles for 500 F are higher than the room temperature values. Other characteristics of the diagrams might be described but it is felt that examination of the graphs will make the salient points obvious.

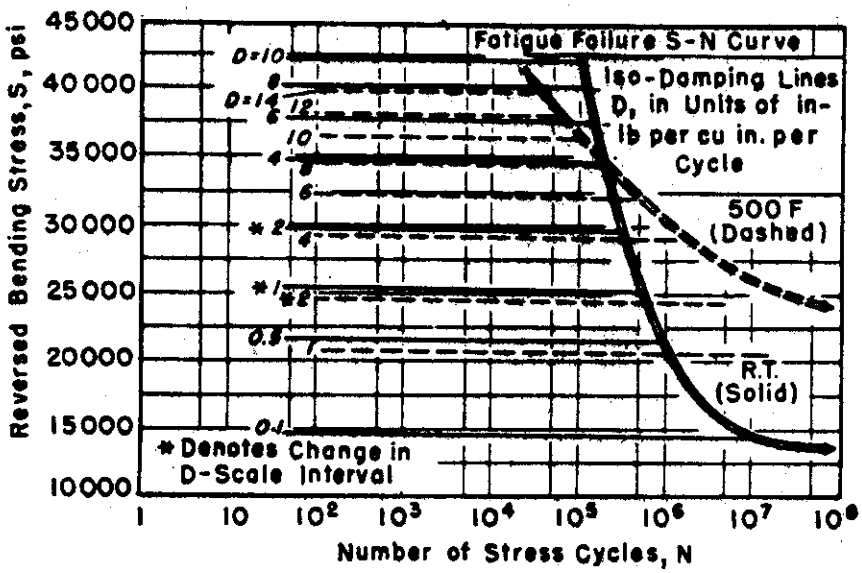

FIG. 18.—*S-N-D* Diagram Relating Stress, Number of Cycles, and Iso-Damping Contour Lines for TP-1-3 (Material H_A) at Room Temperature and 500 F.

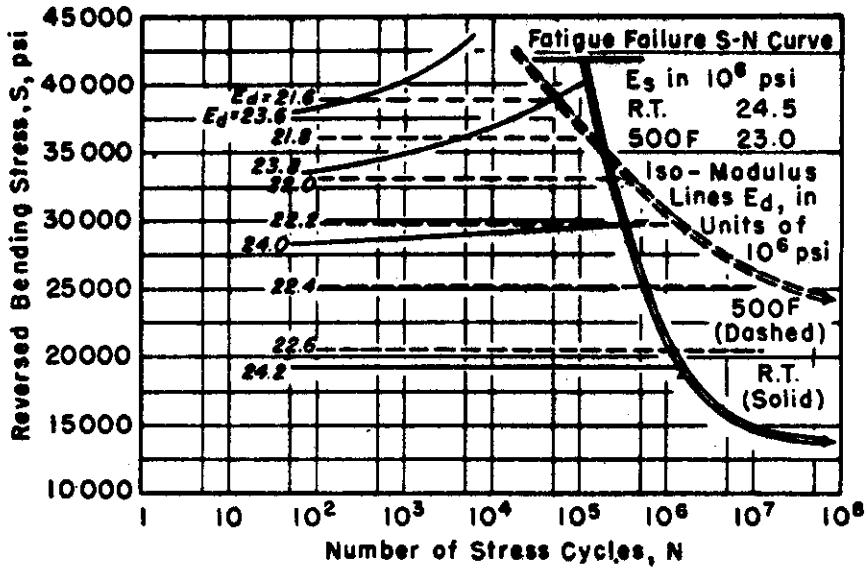

FIG. 19.—*S-N-*E_d Diagram Relating Stress, Number of Cycles, and Iso-Modulus of Elasticity Lines for TP-1-3 (Material H_A) at Room Temperature and 500 F.

Limited data on Inconel X were obtained by testing type Y specimens (solid cylindrical bars, 0.43 in. in diameter by $3\frac{1}{2}$-in. test length, tapered for constant stress). The S-N-D diagram for this material at room temperature is presented in Fig. 20. The dome shaped iso-damping lines indicate a sharp initial decrease in damping followed by a period of no change and then by sharply increasing damping values in the tests run at constant stress. There were no specimens of this material tested at stresses near the long time fatigue strength so the data are all for comparatively short time tests of below 10^5 cycles. The elasticity data for this material are not presented.

Limited data were also procured on the dynamic properties of low carbon N-155 alloy (material NA) at 1500 F. An *S-N-D* diagram is presented in Fig. 21 for this material. The iso-damping lines indicate relatively little change in damping properties during the life of a specimen tested at constant stress.

The actual fatigue *S-N* data which were used in plotting the fatigue curves shown in Figs. 8 through 21 are presented in Fig. 22. The results of the room temperature tests are shown in the first of the two diagrams. The fine lines indicate extrapolated portions of the curves. Although the scatter in the fatigue data is generally relatively small, these data must be considered only approximate since so few specimens were used for each curve. The elevated temperature

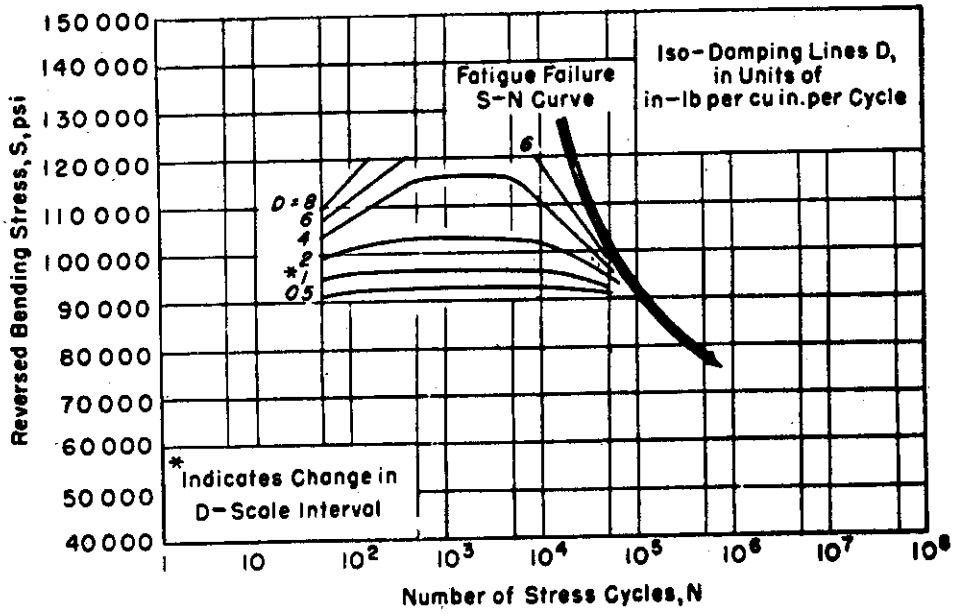

FIG. 20.—*S-N-D* Diagram Relating Stress, Number of Cycles, and Iso-Damping Contour Lines for Inconel X (Material E) at Room Temperature Obtained Using Type Y Specimens (Test Length 3½ in., Average Diameter 0.428 in).

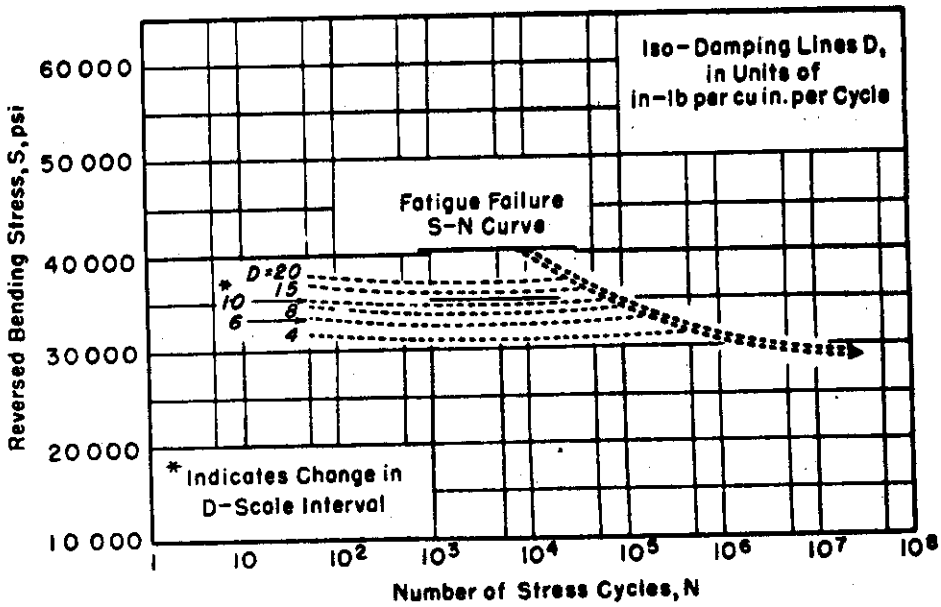

FIG. 21.—*S-N-D* Diagram Relating Stress, Number of Cycles, and Iso-Damping Contour Lines for Low Carbon N-155 Alloy (Material NA) at 1500 F.

fatigue data are presented for type 403, TP-1-2, and TP-1-3 at 500 F; for S-816, TP-2-R, and TP-2-B at 900 F; for N-155 at 1500 F; and for S-816 at 1600 F. In this figure, dashed lines are used for the 500 F data, dotted for 900 F, and dash-dot lines for temperatures above 900 F. One observation made concerning the *S-N* curves of Fig. 22 is that they generally become flatter as the temperature level is raised.

An interesting behavior was that noted for the specimens of S-816 fatigue tested at 1600 F. The specimens did not undergo brittle fracture at the end of a fatigue test, but their stiffness suddenly decreased to such an extent as to allow the loading arm to strike the microswitch and stop the test. Such behavior is not apparent from Fig. 7 since the action occurred so abruptly that no readings were taken immediately preceding the end of a test. This sudden decrease in stiffness did not occur with the same material at 900 F. At this temperature the normal fatigue type of fracture was observed. This was also the case with all of the other elevated temperature speci-

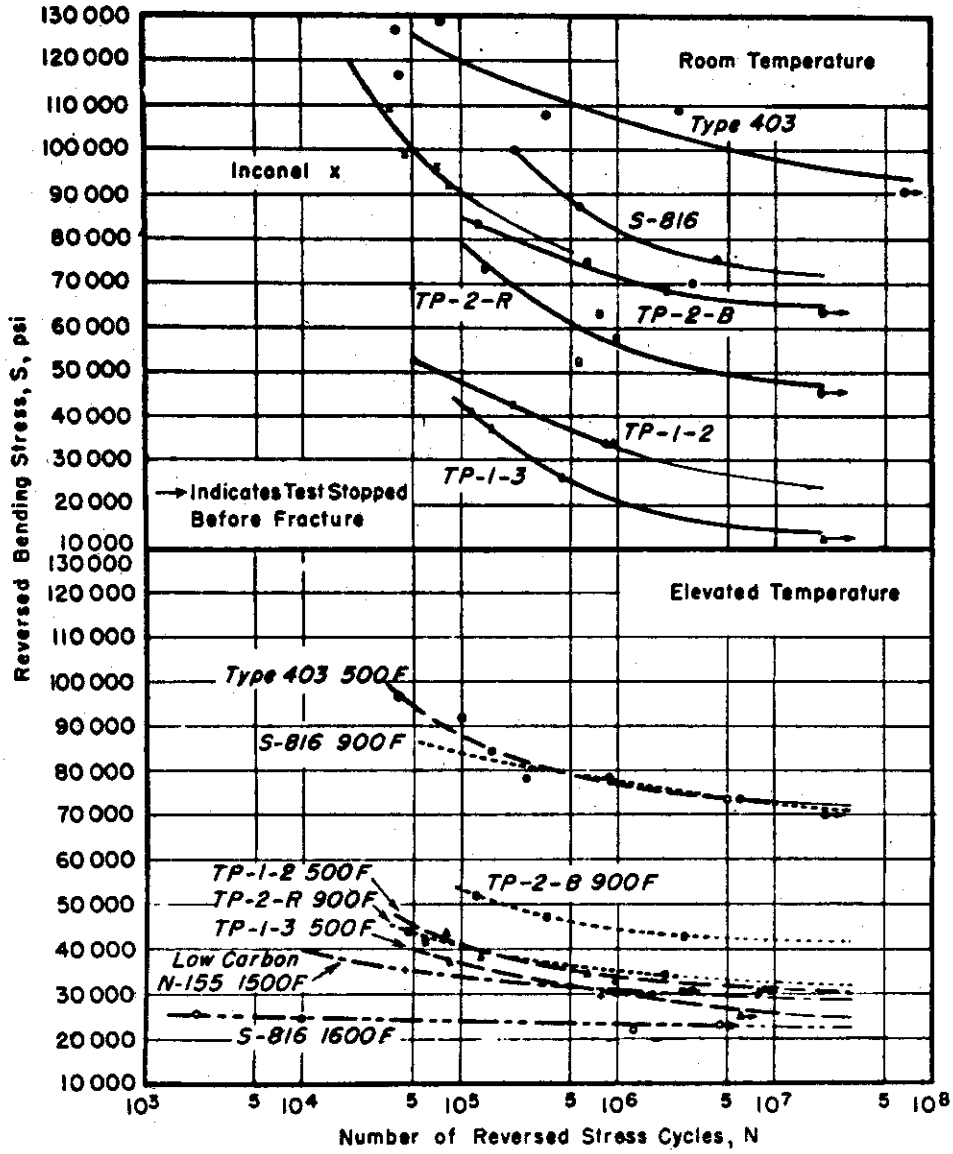

FIG. 22.—*S-N* Fatigue Curves for Various Temperature-Resistant Materials.

mens including those of low carbon N-155 at 1500 F.

A summary of the fatigue strength data obtained in these tests is presented in Table III.

Comparison of the Damping and Fatigue Properties:

When making a choice among several materials for a given dynamic application, not only are the three properties of damping, dynamic modulus, and fatigue strength important individually but also their interrelationships are of considerable engineering significance. In comparing the damping properties of several materials, not only the magnitude of damping energy at a given stress is im-

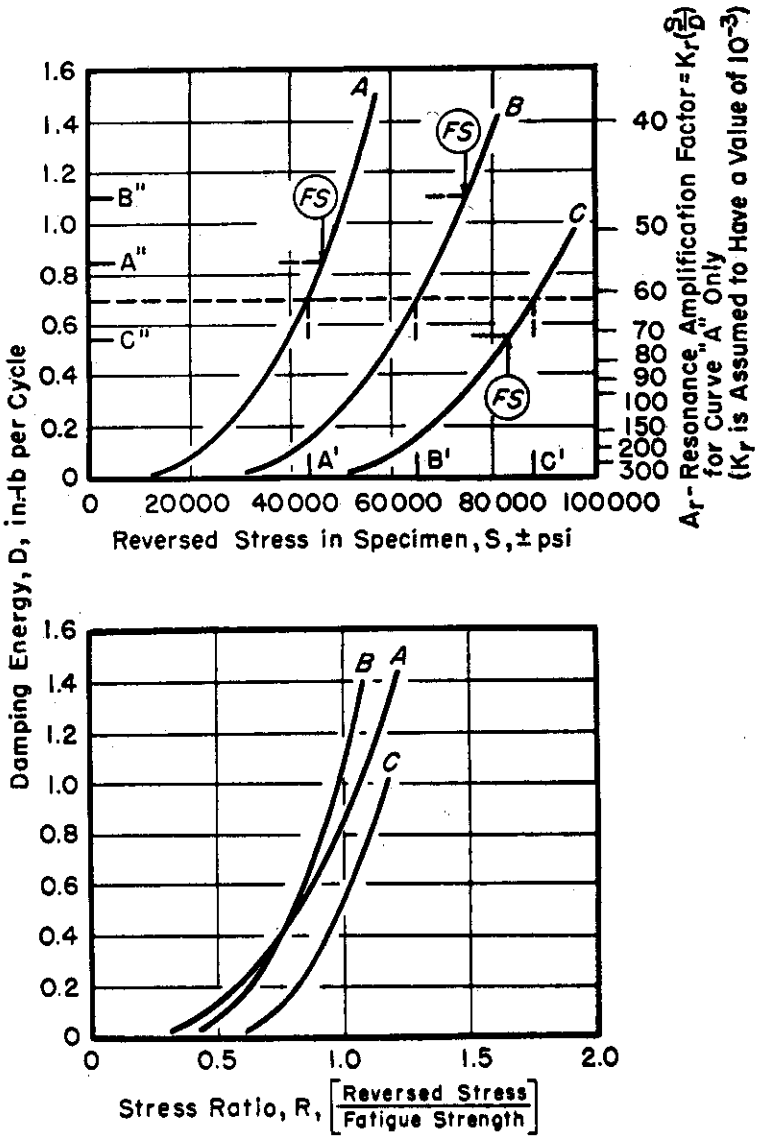

FIG. 23.—Hypothetical Curves for Three Materials Illustrating Methods of Comparing Damping Properties.

TABLE III.—FATIGUE STRENGTHS IN PSI FOR 20 MILLION CYCLES OF REVERSED BENDING STRESS.

Material	Temperature, deg Fahr				
	Room	500	900	1500	1600
S-186	72 000	...	71 500	...	22 500
TP-2-R	47 000	...	32 000	...	...
TP-2-B	65 000	...	42 000	...	...
Type 403	96 000	72 000	...	...	...
TP-1-2	24 000	31 000	...	...	...
TP-1-3	14 000	25 000	...	...	...
Inconel X	57 000[a]	...	...	...	...
Low carbon N-155	...	...	...	29 000	...

[a] Approximate value supplied by Thompson Products Corp.

portant but also the proximity of that stress to the fatigue strengths of the various materials should be considered.

To clarify two methods for comparing the damping properties of a set of materials tested at a given temperature, hypothetical curves for three materials will be discussed. In the upper portion of Fig. 23 are shown curves for three materials A, B, and C which represent a plot to linear scales of damping energy D *versus* stress magnitude S for the three materials after a given number of stress cycles. The damping curves for actual materials do have these general shapes when plotted to linear scales. The flags marked F.S. indicate the fatigue strengths for the materials with C having the highest value and B and A following in that order. On the right side of the figure is indicated a scale for the resonance amplification factor for curve A only, assuming a reasonable value for K_r of 10^{-8}. This factor determines the alternating stress at resonance as given by Eq. 2.

If the damping properties of these three materials are compared on the basis of *equal stress magnitude*, material A would be preferred to material B since it has the greater energy absorption capacity at all values of stress. Likewise, material B would be chosen in preference to material C. However, the relative fatigue strengths of the three materials should also be considered. When operating near resonance, a given machine part may be required to absorb a given amount of input vibrational energy if the near resonance stresses are to be kept within safe limits. Thus, in making a choice of materials for a part subject to near resonance service, comparison should be made on the basis of equal energy absorbed rather than on the basis of equal stress. The amplitude of vibration and, therefore, the stress would increase until the energy dissipated through damping was equal to the vibrational energy input. For example, with the three materials under consideration, suppose that the amount of energy required to be absorbed by the material is 0.7 in-lb per cycle. A horizontal line drawn at this value of damping energy in the upper diagram of Fig. 23 indicates the three materials would be operating at stresses shown by values A′, B′, and C′ respectively on the abscissa. In comparing these stresses with the co-responding fatigue strengths, material A operates slightly below its fatigue strength, material B considerably below, and material C would be significantly above its fatigue strength.

In order to clarify further the relationship between damping and fatigue behaviors, the damping data for the three materials A, B, and C are replotted as shown in the lower portion of Fig. 23. In this graph, the abscissa is the ratio of the reversed stress to the fatigue strength of the material. At stresses corresponding to their fatigue strengths, materials A, B, and C have damping energy values as given by A″, B″, and C″ in the upper portion of Fig. 23. These values are plotted in the lower diagram at a stress ratio of 1.0. In comparing the relative damping properties of the three materials in this manner, material C is the least effective energy absorber. Material A has the highest damping at low stress ratios, but material B exhibits superior properties to A for values of stress ratio in excess of 0.75.

The foregoing discussion is not meant to imply that a material of high fatigue strength is always inferior with respect to damping when compared on the basis of stress ratio with materials of lower fatigue strengths (see Reference (3) for example). On the contrary, in many cases materials of high fatigue strength often exhibit higher damping capacity at stress

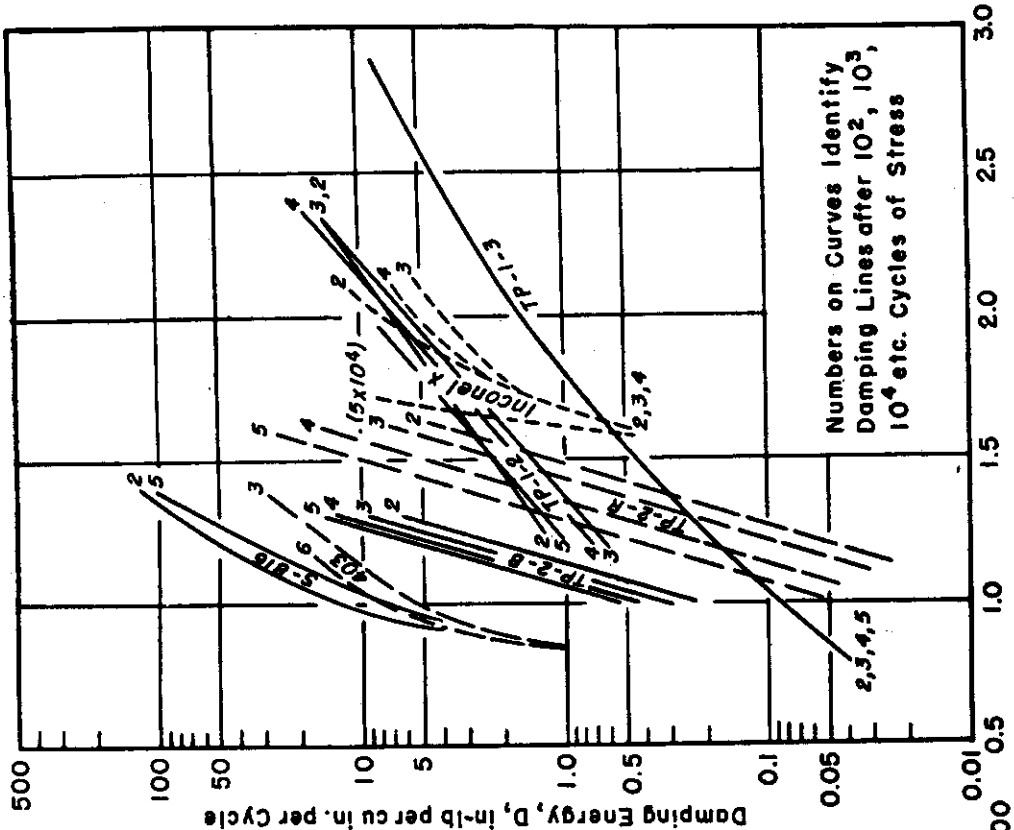

FIG. 25.—*D-R-N* Diagrams for Several Temperature-Resistant Materials Comparing Damping Energy at Room Temperature as a Function of Stress History and Stress Ratio.

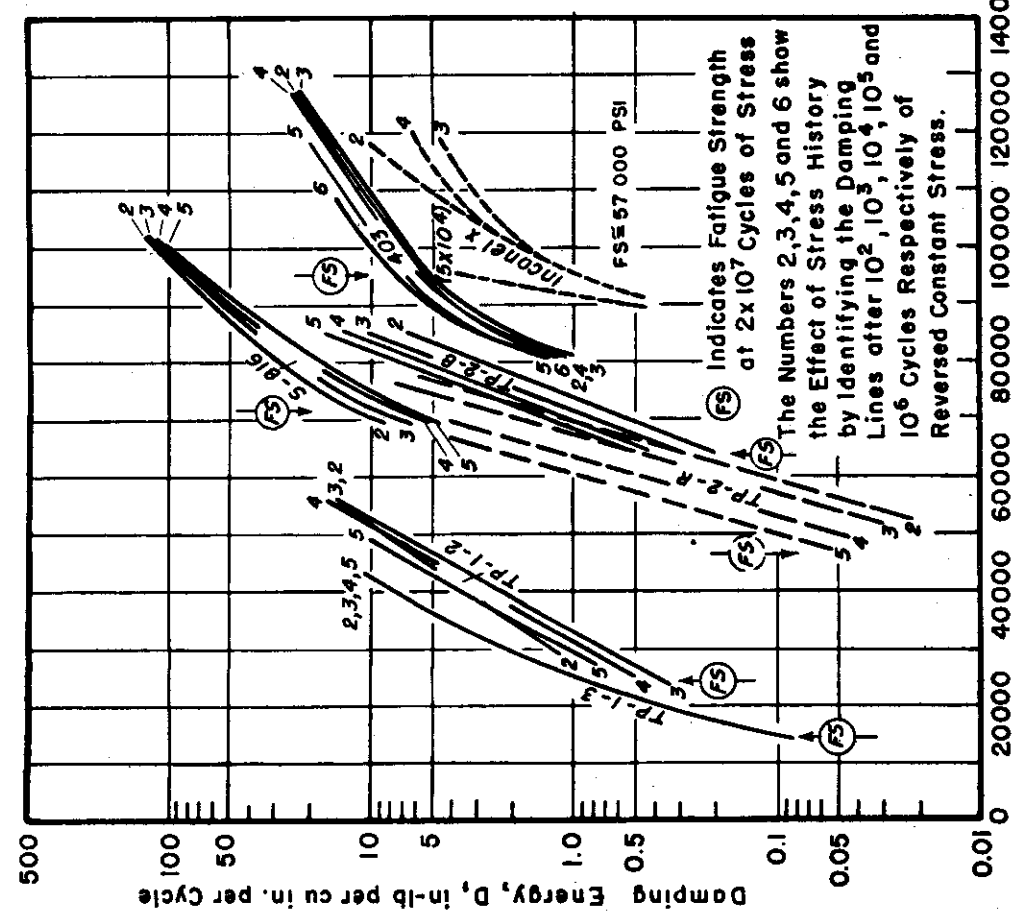

FIG. 24.—*D-S-N* Diagrams for Several Temperature-Resistant Materials Comparing Damping Energy at Room Temperature as a Function of Stress History and Stress Magnitude.

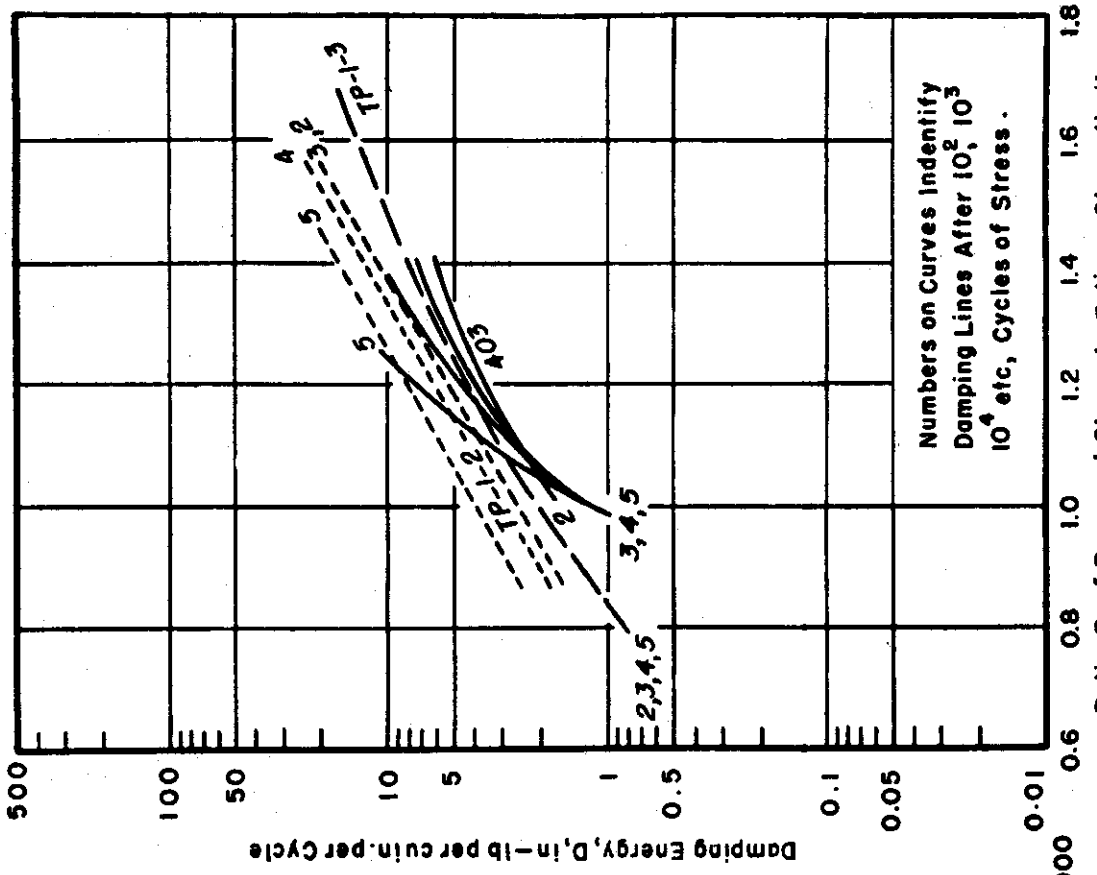

FIG. 27.—*D-R-N* Diagrams for 403, TP-1-2, and TP-1-3, Comparing Damping Energy at 500 F as a Function of Stress History and Stress Ratio.

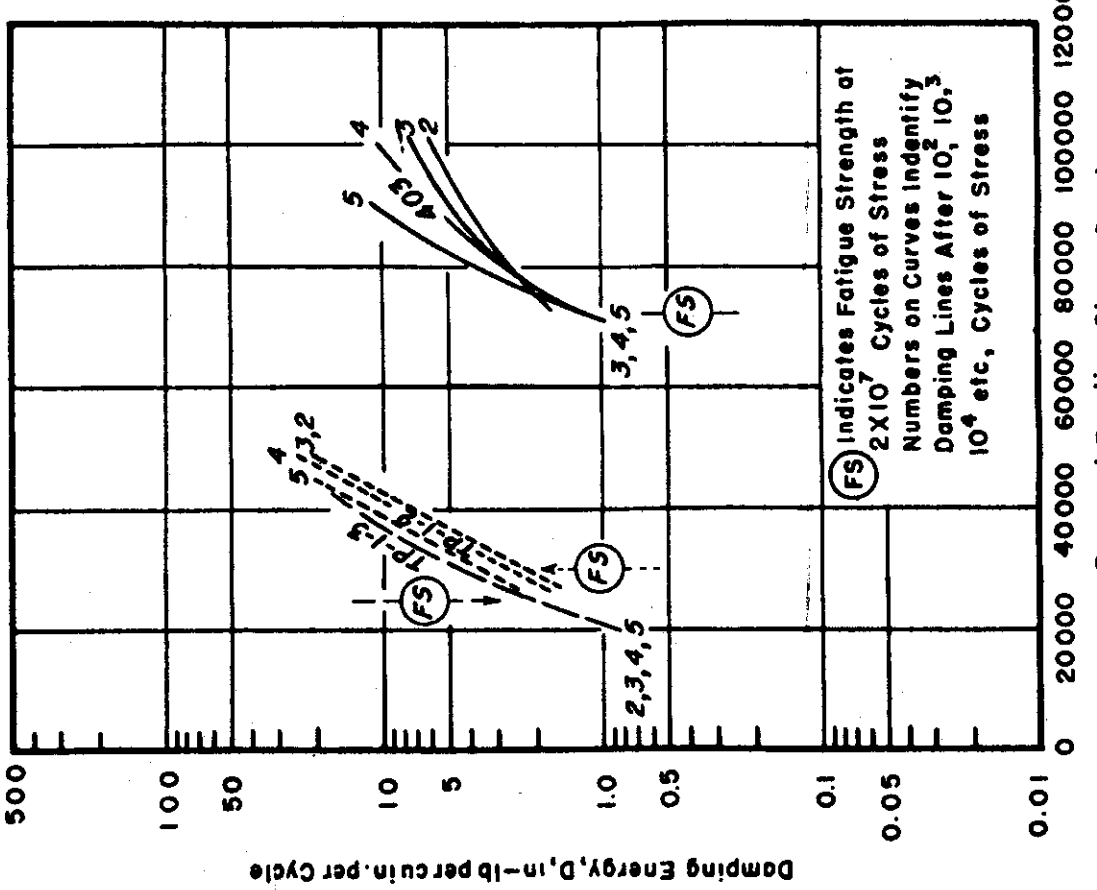

FIG. 26.—*D-S-N* Diagrams for 403, TP-1-2, and TP-1-3 Comparing Damping Energy at 500 F as a Function of Stress History and Magnitude.

ratios of 1.0 than do the dynamically weaker materials.

A third factor not mentioned in this discussion of the comparison of damping properties is the effect of stress history. The hypothetical curves drawn in Fig. 23 apply to a fixed stress history. However, one material might have decreasing damping values with increasing number of cycles at stress while another might have the opposite trend so that a given material could be inferior to another after 100 cycles of stress, yet be considerably superior after exposure to, say, 100,000 cycles.

A comparison of materials tested in this program on the basis of the same stress magnitude is given in Figs. 24, 26, and 28. These graphs are similar to the upper diagram in Fig. 23. They show damping energy, D, plotted to a log scale as a function of reversed bending stress, S, with iso-history contour lines connecting the damping values after a given number N of reversed constant stress cycles. They are termed D-S-N diagrams. Similar graphs comparing the damping of materials on the basis of stress ratio rather than stress magnitude are termed D-R-N diagrams. The R indicates the ratio of the reversed stress to the fatigue strength of the material. Diagrams of this type for the materials tested in this program are shown in Figs. 25, 27, and 29.

A comparison of the room temperature damping properties on the basis of the same stress magnitude is presented in Fig. 24 for all of the materials tested at room temperature. The fatigue strength at 20 million cycles of stress is indicated for each material by a flag marked F.S. Iso-history contour lines are marked by 2, 3, 4, etc., to indicate the damping after 10^2, 10^3, 10^4, etc., stress cycles. The data for all materials except Inconel X were obtained using type E specimens. For that material a larger specimen was employed as described in the discussion of the S-N curves. It is observed in Fig. 24 that the relative damping energy values among a group of materials at a given stress vary in a general way inversely as their fatigue strengths. For example, the TP-1 materials have the lowest fatigue strengths; yet at a given stress value, they display greater damping than the dynamically stronger materials. Inconel X is one major exception to this behavior for, although possessing an intermediate value of fatigue strength, its damping at a given stress is about the lowest of all the materials. It is improbable that the larger size specimens used for Inconel X can explain this nonconformity.

The effects of stress history on the damping properties of the various materials are also apparent from this diagram. Thus, materials TP-1-2, TP-2-R, TP-2-B, and type 403 are seen to have generally increasing damping with an increase in number of cycles at constant stress; S-816 displays the reverse tendency; the damping of TP-1-3 as noted previously is unaffected by stress history; and Inconel X displays a combination of the above trends. The room temperature damping properties of TP-2-R and Inconel X are more affected by stress history than those of the other materials.

The damping properties of the same seven materials at room temperature are compared on the basis of stress ratio by means of the D-R-N diagrams of Fig. 25. Many of the features discussed in connection with the lower diagram of Fig. 23 are displayed by these groups of curves. The damping of type 403 which is inferior to that of most of the other materials on the basis of the same stress (Fig. 24) is seen to be many times greater than that of any of the other materials except S-816 when compared at a stress ratio of one. Alloy S-816 displays unusual properties in that its damping capacity com-

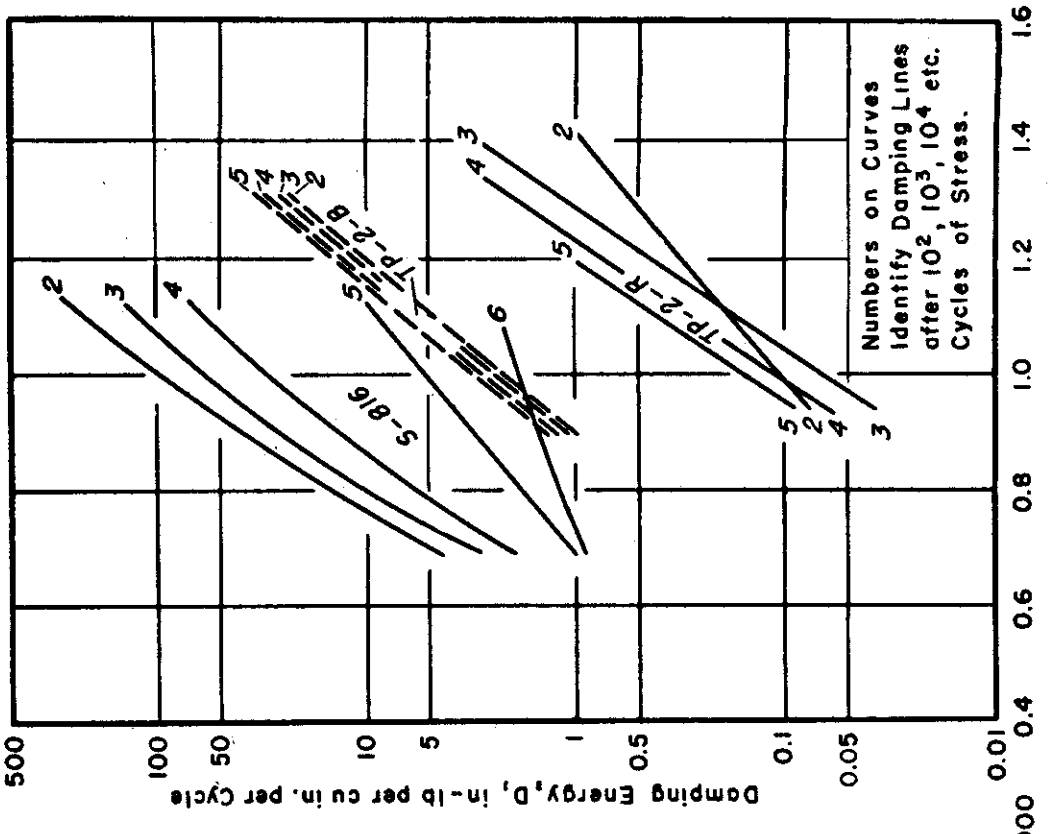

FIG. 29.—*D-R-N* Diagrams for S-819, TP-2-R, and TP-2-B, Comparing Damping Energy at 900 F as a Function of Stress History and Stress Ratio.

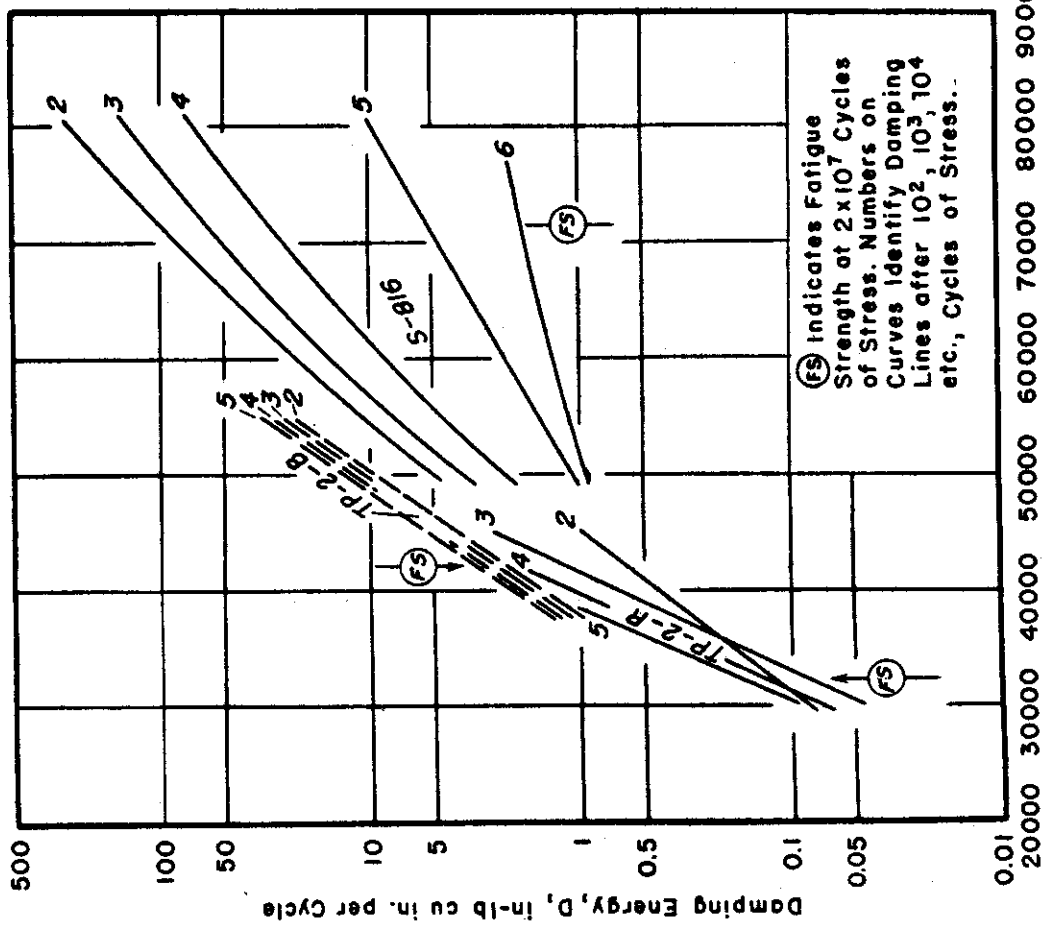

FIG. 28.—*D-S-N* Diagrams for S-816, TP-2-R, and TP-2-B, Comparing Damping Energy at 900 F as a Function of Stress History and Stress Magnitude.

pares favorably with the other materials on the basis of equal stress and is also superior to all of those tested (except type 403 after a large number of cycles) when compared on the basis of the same stress ratio. The TP-1 materials have a tendency to display damping values superior to all of the other materials tested for low stress ratios. The effect of different heat treatments on the same powder metal is shown by comparing the curves for TP-1-2 with those for TP-1-3. It is also interesting to compare the curves for TP-2-B, the arc-cast molybdenum plus 2 per cent tungsten material, with those for TP-1-2, sintered iron powder. They have similar damping values for a stress ratio of one, yet the curves have sharply different slopes. The combined effects of a different method of manufacture and a difference in composition are seen in comparing the curves for TP-2-B and TP-2-R.

The relative order of merit for the damping properties of a group of materials may be the same at elevated temperature as at room temperature or it may be considerably different. Obviously, then, the damping of materials should be determined at the temperature of service. In comparing the room temperature damping properties of the three materials, type 403 stainless (extrapolated to low stress values), TP-1-2, and TP-1-3 on the basis of magnitude of reversed stress (see Fig. 24), the two powder metals display considerably higher damping at a given stress. As seen in Fig. 26, the same general relationships hold true for the properties at 500 F with the damping values for the powder metals being considerably higher than those for the wrought type 403 for stresses in the range of 20,000 to 50,000 psi. After 100,000 cycles of stress, the curves for the two TP-1 materials are very close to each other.

When the same three materials are compared on the basis of stress ratio, however, as in Fig. 27, it is seen that the values for the wrought and powder metals are much closer together. For a large number of stress cycles, the damping values for TP-1-2 are greater than those of TP-1-3 at all stress ratios. Both of these materials exhibit somewhat higher damping values than type 403 at a stress ratio of one, but after a large number of stress cycles at the higher stress ratios, the damping of type 403 becomes the greatest.

Figures 28 and 29 compare the 900 F damping properties of materials S-816, TP-2-B, and TP-2-R. On the basis of the same magnitude of applied stress, Fig. 28 indicates that TP-2-B absorbs greater energy than either of the other two materials at stress values below 40,000 psi. Due to the greater rate of change of damping with stress, TP-2-R displays higher damping values after a large number of stress cycles at stresses greater than about 40,000 psi than either S-816 or TP-2-B. The relative effects of stress history on the damping properties of the three materials are apparent from this plot. S-816 is affected far greater by stress history than either of the other two materials.

Since the fatigue strengths of the three materials tested at 900 F vary widely, the plot of damping as a function of stress ratio shown in Fig. 29 is an interesting one. If a comparison is made at a stress ratio of one, S-816 after 100 cycles of stress displays a damping energy about 40 times that of TP-2-B and about 1000 times that of TP-2-R. After 100,000 cycles of stress, however, the damping of S-816 is less than twice that of TP-2-B and only about 25 times that of TP-2-R. After a greater number of cycles of stress, the damping of S-816 falls below that of TP-2-B, but is still greater than that of TP-2-R. At values of stress ratio less than about 0.8, S-816 displays higher

damping than either of the other two materials.

No attempt is made in this paper to express mathematically the relationships among damping energy, stress, and stress history. It should be mentioned however, that logarithmic plating of damping *versus* stress result reasonably straight lines in many cases and damping may be related to stress by the expression:

$$D = QS^n$$

where Q and n are constants. The range of exponent n for the materials tested is from 2 to 30.

Comparison of the Elasticity Properties:

In Fig. 30 are presented E_d - S-N diagrams for six of the materials tested at room temperature. This graph shows dynamic modulus of elasticity E_d as a function of reversed bending stress, S, with lines connecting the dynamic modulus of elasticity values after a given number N of reversed constant stress cycles. The horizontal dashed lines indicate the static modulus values for the virgin specimens. The F.S. flags have their usual meaning. It should be noted that for room temperature the differences between the dynamic moduli and the static moduli are small for stresses up to the fatigue strength of a material. S-816 displays the greatest decrease in modulus value at the fatigue strength in which case after 100 cycles of stress there is a decrease of somewhat less than 3 per cent from the virgin static value. At stresses in excess of the fatigue strength of a given material, the decrease in stiffness is in some cases appreciable. For example, for TP-2-R after 100,000 cycles at a stress approximately 1.5 times its fatigue strength, there is a decrease to about 90 per cent of the initial static modulus. Even this 10 per cent decrease is considerably smaller than that observed for mild steel (1), which is 35 per cent at a stress ratio of 1.16. Stress history seems to have small effect on the dynamic modulus of TP-1-3 and perhaps the greatest effect on that of TP-2-R.

Figure 31 shows the E_d-S-N diagrams for the same six materials at elevated temperatures: 500 F for the TP-1 materials and type 403; 900 F for the TP-2 materials and S-816; and 1600 F for S-816. The method of plotting is identical with that of Fig. 30. The dynamic moduli values at stresses corresponding to the elevated temperature fatigue strengths are only a few per cent different (usually lower) than the virgin static moduli at the same temperature for all materials and all temperatures investigated except in the case of S-816 at 900 F. As pointed out previously in connection with Fig. 9, both stress magnitude and stress history exert a large effect on the dynamic modulus of S-816 at this temperature. For example, to show the effect of stress history, at a stress corresponding to the 900 F fatigue strength of S-816, the dynamic modulus after 100 cycles of stress is about 80 per cent of the initial static modulus. After 1,000,000 cycles of stress, the dynamic modulus value is about 102 per cent of the initial static value. Observing the effect of stress magnitude, it is seen that at a stress of 50,000 psi after 100 cycles the dynamic modulus has a value about 98.5 per cent of the initial static value while at 80,000 psi after the same number of cycles its value is only 71 per cent of the initial static value. Both stress magnitude and stress history exert an appreciable effect on the dynamic modulus of the TP-2 materials at 900 F for stresses considerably in excess of the fatigue strengths of the materials. The effects of these two variables are less pronounced in the case of the materials tested at 500 F. Material TP-1-3 remained unaffected by stress history at 500 F, a behavior similar to that displayed at room temperature at low stress.

The absolute value of the modulus of

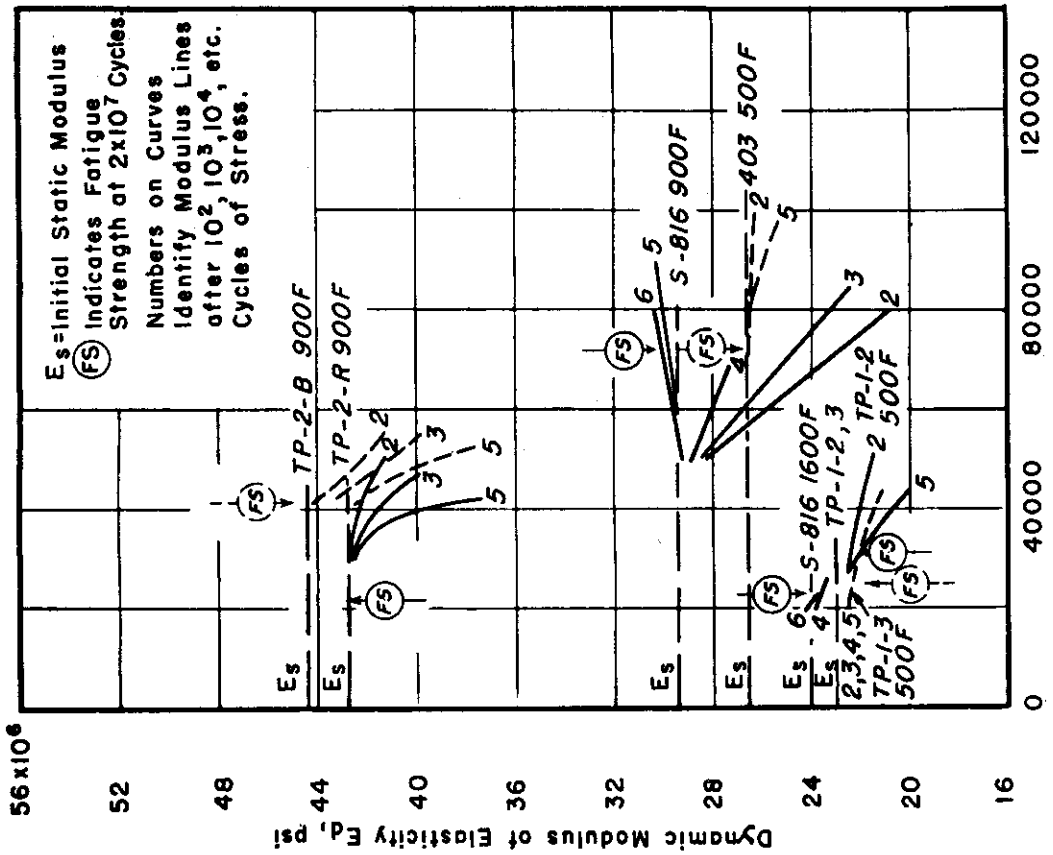

FIG. 31.—E_d-S-N Diagrams for Several Temperature-Resistant Materials Comparing Dynamic Modulus of Elasticity at Elevated Temperatures as a Function of Stress History and Stress Magnitude.

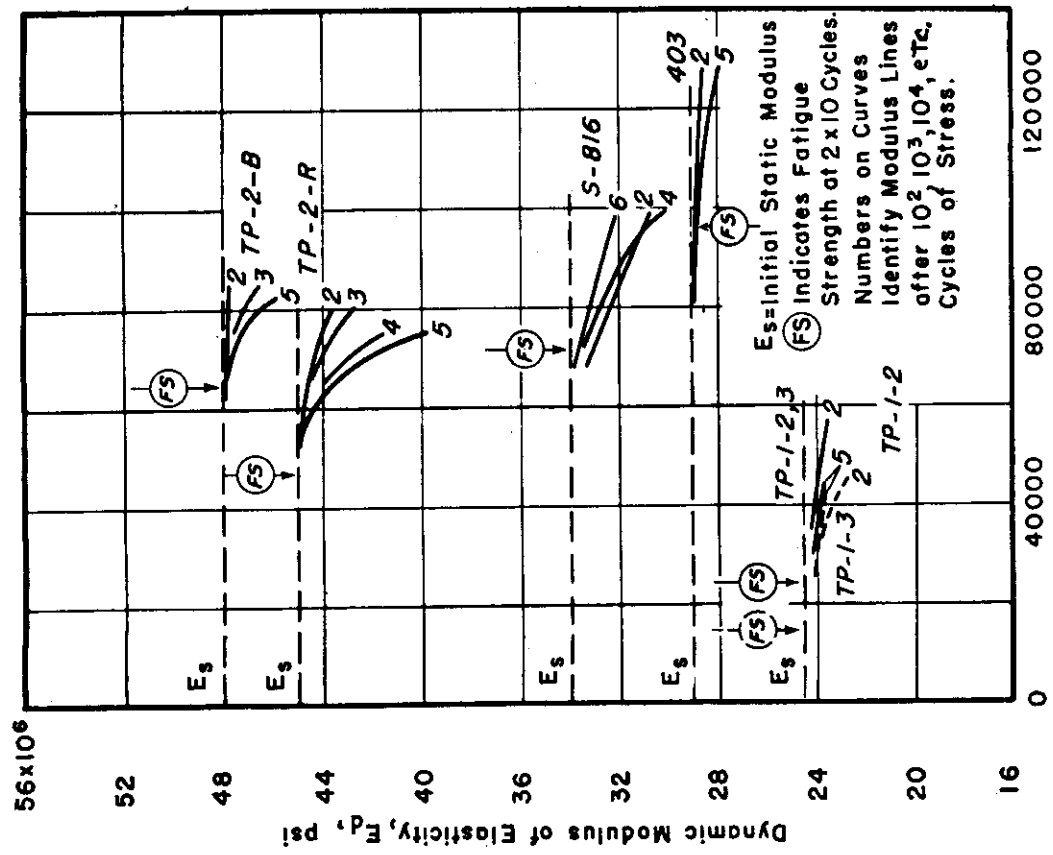

FIG. 30.—E_d-S-N Diagrams for Several Temperature-Resistant Materials Comparing Dynamic Modulus of Elasticity at Room Temperature as a Function of Stress History and Stress Magnitude.

elasticity of a material at operating temperature is a major factor in determining the natural frequency of a blade made of that material. The use of the natural frequencies in machine design was discussed previously in this paper. For a very rough comparison of materials, it may be assumed that as a first approximation the natural frequency is proportional to the square root of the modulus of elasticity of the material. The relative frequencies of a given blade made of different materials may then be compared by using the second roots of the moduli of elasticity of the materials assuming the masses of the different blades to be the same. Such a comparison may be made among the materials tested at the same temperature by using the square roots of the static values of elastic modulus given in Table II. This table gives the static moduli of elasticity for the materials tested at the various temperatures. The static values may be used since relatively little change from these values was observed with cyclic stress history for stress values near the fatigue strengths of the materials. The one major exception to this is, of course, S-816 at 900 F which even at a stress equal to the fatigue strength has dynamic modulus values displaying major deviations from the initial static modulus. The natural frequency of a blade made from this material and subjected to a cyclic stress equal to its fatigue strength would, at this temperature, be affected greatly by the stress history of the blade.

TABLE IV.—COMPARISON OF APPROXIMATE RELATIVE AMPLITUDES AT RESONANCE.

Material	Cyclic Stress to Produce Damping of 5 in-lb per cu in. per cycle After 10^8 Cycle of Stress, psi	E_d at 10^8 Cycles, psi	Unit Strain, S/E_d, in. per in.
Room Temperature			
S-816	70 000	33 700 000	0.00208
TP-2-R	67 500	43 100 000	0.00156
TP-2-B	78 000	46 900 000	0.00166
Type 403	80 500	28 800 000	0.00279
TP-1-2	43 000	23 700 000	0.00181
TP-1-3	36 500	23 800 000	0.00153
500 F			
Type 403	82 000	26 300 000	0.00311
TP-1-2	33 000	21 900 000	0.00151
TP-1-3	31 000	22 100 000	0.00140
900 F			
S-816	71 000	29 800 000	0.00238
TP-2-R	44 500	34 000 000	0.00131
TP-2-B	44 000	41 900 000	0.00105

It would be impossible to determine the desirability of one material with respect to another as far as the relative blade stiffness properties are concerned unless machine design data were available and natural frequency calculations (9) made for blades of each material. With this information the location of the critical frequency spectrum, with respect to the operating speed range of the machine, would be known for blades of each material. For the frequency calculations, elevated temperature moduli should be used. Since the temperatures vary at different stations along the length of the blade, the modulus values should be known for a range of elevated temperatures. The variation of the dynamic moduli with stress and with stress history for the different materials as given in Figs. 30 and 31 will afford an indication of the amount of change that can be expected in the natural frequency of a given blade made of various materials when operating under various conditions at the temperatures indicated.

The last consideration to be discussed relative to stiffness properties is that of a comparison among a group of materials for the amplitude of vibration when passing through or operating at a resonant frequency. This comparison should be made on the basis of equal energy dissipation since materials of differing damping properties must be subjected to cyclic stress of different magnitudes to pro-

duce the same energy dissipation. These stresses produce different values of deflection in blades made of various materials depending on the elasticity properties of those materials. Such a comparison is presented in Table IV. The data for column 2 of this table were obtained from Fig. 5 for S-816 and similar *D-S-N* plots for the other materials. The value of 5 in-lb per cu in. per cycle and the number of stress cycles (10^5) were arbitrarily chosen to obtain values for comparison. The E_d values of column 3 were read from large scale E_d-*S-N* diagrams similar to Figs. 30 and 31. The values in column 4 may be used to determine the relative amplitudes of deflection for similar blades made from different materials. Thus, at a resonance for which the vibrational energy input to the material itself is 5 in-lb per cu in per cycle, the deflection at 500 F of a blade made of type 403 would be more than twice that of a blade made of TP-1-2. Similarly, a blade made of S-816 would have a deflection at resonance greater than twice that of one made of TP-2-B when dissipating the same amount of energy at 900 F. It is also interesting to note that the unit strains (or relative amplitudes) of S-816 and type 403 increase upon going from room temperature to an elevated temperature whereas the values for the other four materials have the opposite trend. In applications where deflections are limited by the design of the machine, then such factors as discussed above are important in materials selection.

TABLE V.—QUALITATIVE RATINGS[a] OF MATERIALS AT ROOM AND ELEVATED TEMPERATURES.

Material	Fatigue Strength		Damping Capacity for Stress Ratio of 1.0		Least Deflection at Resonance for Blade of a Given Material	
	RT	500 F	RT	500 F	RT	500 F
Type 403...	1	1	1	3	3	3
TP-1-2.....	2	2	2	1	2	2
TP-1-3.....	3	3	3	2	1	1
	RT	900 F	RT	900 F	RT	900 F
S-816.....	1	1	1	1 or 2[b]	3	3
TP-2-R.....	3	3	3	3	1	2
TP-2-B.....	2	2	2	1 or 2[b]	2	1

[a] 1, 2, and 3 indicate decreasing order of merit with respect to a given property.
[b] Rating is dependent upon stress history.

The comparison of resonant vibration amplitude discussed above is important not only in considering clearance and other design factors, but it may also indicate the volume of noise produced during resonant conditions. Thus, column 4 of Table IV may be significant in selecting materials for applications where noise must be kept at a low level.

Materials Selection:

In previous sections, the fatigue, damping capacity, and modulus of elasticity properties for groups of materials have been compared and evaluated separately in a quantitative fashion. A qualitative rating of the materials in a group according to the three properties for the two test temperatures is shown in Table V to facilitate materials selection. Table V was prepared from Figs. 22 through 31. It is obvious that while room temperature tests may indicate the relative rating at elevated temperatures with respect to one property, they may be misleading with respect to other properties.

For the final evaluation of materials for a given application, a table such as Table V can be set up with other columns for properties which also affect service behavior such as creep, resistance to oxidation, ductility, etc. Each material could be rated separately according to each property and then, if the relative importance of these properties is known for a given application, a final over-all figure of merit for each material could be determined. This index of serviceability,

considered along with availability, cost, workability, etc., would govern materials selection.

Summary and Conclusions

Damping capacity, dynamic modulus of elasticity, and fatigue strength properties are of great importance in the design of parts used in applications involving dynamic loads. Data are reported in this paper on the results of room and elevated temperature tests designed to reveal changes in the damping and elasticity properties of various materials during constant reversed cyclic stress tests at engineering stress levels. Newly developed rotating-cantilever beam fatigue-testing equipment was used in this work.

Data for S-816 at room temperature 900 F, and 1600 F; for TP-2-R and TP-2-B at room temperature and 900 F; for type 403 TP-1-2, and TP-1-3 at room temperature and 500 F; for Inconel X at room temperature; and for low carbon N-155 at 1500 F, presented in a series of new diagrams, show the dependence of the damping and elasticity properties upon both stress magnitude and stress history and facilitate comparison and evaluation of these properties. Various patterns have been observed in the behavior of these properties during constant stress tests carried out at various temperatures. For all materials and at all temperatures investigated, the energy dissipated by damping increases rapidly with stress at values close to the fatigue strength of a material. During a constant reversed cyclic stress test, the damping energy may decrease, remain the same, increase, or have a varying pattern as the number of stress cycles is increased. In general, the changes in dynamic modulus of elasticity are reciprocal to the changes in damping energy.

Room and elevated temperature *S-N* data presented for the various materials indicate that, in general, the curves tend to become flatter as the temperature level is raised. The elevated temperature fatigue strengths for temperature resistant materials may be lower, equal to, or greater then the room temperature values.

Two methods for comparing the damping and elasticity properties of materials are presented and the merits of each discussed. The first is on the basis of equal stress magnitude and the second is on the basis of the same ratio of applied stress to fatigue strength. The latter method should be employed in applications where resonant vibrations are encountered since the service requirement is a given amount of energy absorbed rather than a definite stress applied. Special diagrams presented facilitate a comparison of the damping properties for each of the methods outlined above. Evaluations of the damping properties are made for the groups of materials tested at the same elevated temperatures.

Figures 30 and 31 for room temperature and elevated temperature tests facilitate comparison of the elasticity properties. They show the dependence of the dynamic modulus of each material upon stress magnitude and stress history. The square roots of the moduli of elasticity reported in Table II provide an indication of the approximate relative natural frequencies of vibration of turbine or compressor blades made of the various materials. Table IV shows the approximate relative deflections obtained at resonance for blades made of various materials.

Table V outlines a method for comparing different materials on the basis of their dynamic properties: damping, elasticity, and fatigue strength.

In conclusion, it is felt that the new diagrams and tables for explanation and

evaluation of the behavior of the dynamic properties of materials and the new and revealing data presented may aid in the comprehension of one of the least understood of the dynamic properties, damping, and emphasize the large changes which may take place in another, dynamic modulus of elasticity. It is hoped that the methods for the comparison and evaluation of materials will be of value either in selecting a material for a new application, or for rating replacement materials by comparing their properties with those of materials which have already proved their worth in a given application.

Acknowledgment:

The fine cooperation and encouragement of the Office of Naval Research, Thompson Products Corp. and the U. S. Air Force, sponsors of this work, are greatly appreciated.

All of the test specimens except N-155 were furnished in the form for final polishing by Thompson Products Corp. Specimens of N-155 were furnished in final form by the National Advisory Committee for Aeronautics.

S. Tomkinson, G. Gronau, M. Linza, and P. Madonna assisted in the development of the machines and in the preparation and testing of the specimens.

References

(1) B. J. Lazan, "A Study With New Equipment of the Effects of Fatigue Stress on Damping Capacity and Elasticity of Mild Steel," *Transactions*, Am. Soc. Metals, Vol. 4, pp. 499–558 (1950).

(2) J. M. Robertson and A. J. Yorgiadis, "Internal Friction in Engineering Materials," *Journal of Applied Mechanics*, Vol. 13, pp. A173–A181.

(3) B. J. Lazan and A. J. Yorgiadis, "The Behavior of Plastics Under Repeated Stress," Symposium on Plastics, Am. Soc. Testing Mat., pp. 66–94 (1944).

(4) B. J. Lazan and T. Wu, "Damping, Fatigue, and Dynamic Stress-Strain Properties of Mild Steel," *Proceedings*, Am. Soc. Testing Mats., Vol. 51 (1951).

(5) I. Perlmutter, "Service Failures of Turbine Buckets," Air Force Technical Report No. 5716, July, 1948.

(6) B. J. Lazan, "Some Mechanical Properties of Plastics and Metals Under Sustained Vibrations," *Transactions*, Am. Soc. Mechanical Engrs., Vol. 65, pp. 87–104 (1943).

(7) O. Föppl, "The Practical Importance of Damping Capacity of Metals, Especially Steels," *Journal*, Iron and Steel Inst., Vol. 134, pp. 393–455 (1936).

(8) B. J. Lazan, "Dynamic Creep and Rupture Properties of Temperature-Resistant Materials Under Tensile Fatigue Stress," *Proceedings*, Am. Soc. Testing Mats., Vol. 49, pp. 757–798 (1949).

(9) A. Herzog, "Calculations of Natural Frequencies and Stresses, and Proposed Testing Methods," Air Force Technical Report No. 5936, Part I, May, 1950.